สารยับยั้งเอนไซม์แอลฟากลูโคซิเดสจากอนุพันธ์อะมิโนไซคลิทอล

นางสาววิศุษฎญา วรวะลัย

วิทยานิพนธ์นี้เป็นส่วนหนึ่งของการศึกษาตามหลักสูตรปริญญาวิทยาศาสตรมหาบัณฑิต
สาขาวิชาเคมี ภาควิชาเคมี
คณะวิทยาศาสตร์ จุฬาลงกรณ์มหาวิทยาลัย
ปีการศึกษา 2551

α-GLUCOSIDASE INHIBITORS FROM AMINOCYCLITOL DERIVATIVES

Miss Wisuttaya Worawalai

A Thesis Submitted in Partial Fulfillment of the Requirements
for the Degree of Master of Science Program in Chemistry
Department of Chemistry
Faculty of Science
Chulalongkorn University
Academic Year 2008

Thesis Title	α-GLUCOSIDASE INHIBITORS FROM AMINOCYCLITOL DERIVATIVES
By	Miss Wisuttaya Worawalai
Field of Study	Chemistry
Advisor	Assistant Professor Preecha Phuwapraisirisan, Ph.D.
Co-Advisor	Sumrit Wacharasindhu, Ph.D.

Accepted by the Faculty of Science, Chulalongkorn University in Partial Fulfillment of the Requirements for the Master's Degree

S. Hannongbua ..... Dean of the Faculty of Science

(Professor Supot Hannongbua, Dr.rer.nat.)

THESIS COMMITTEE

Sirirat Kokpol ..... Chairman

(Associate Professor Sirirat Kokpol, Ph.D.)

Preecha Phuwapraisirisan ..... Advisor

(Assistant Professor Preecha Phuwapraisirisan, Ph.D.)

..... Co-Advisor

(Sumrit Wacharasindhu, Ph.D.)

A. Shitangkoon ..... Examiner

(Assistant Professor Aroonsiri Shitangkoon, Ph.D.)

Wimolpun Rungprom ..... External Examiner

(Assistant Professor Wimolpun Rungprom, Ph.D.)

วิศุษฎญา วรวะลัย : สารยับยั้งเอนไซม์แอลฟากลูโคซิเดสจากอนุพันธ์อะมิโนไซคลิทอล. (α-GLUCOSIDASE INHIBITORS FROM AMINOCYCLITOL DERIVATIVES) อ.ที่ปรึกษาวิทยานิพนธ์หลัก : ผศ.ดร.ปรีชา ภูวไพรศิริศาล, อ.ที่ปรึกษาวิทยานิพนธ์ร่วม : อ.ดร.สัมฤทธิ์ วัชรสินธุ์, 58 หน้า.

ได้ศึกษาการสังเคราะห์ที่มีประสิทธิภาพของอนุพันธ์อะมิโนไซคลิทอลที่เป็นคู่ไดแอสเตอริโอเมอร์ 2 ชนิด คือ 5*S*-amino-1,2,3,4-cyclohexanetetrol และ 5*R*-amino-1,2,3,4-cyclohexanetetrol พร้อมทั้งทำการสังเคราะห์อนุพันธ์เคอร์ซิทอลชนิดอื่น โดยสารตั้งต้นที่ใช้ในการสังเคราะห์ครั้งนี้ คือ (+)-*proto*-quercitol ซึ่งเป็นสารที่แยกได้จากธรรมชาติ ด้วยความเหมาะสมทางด้านสเตอริโอเคมีของ (+)-*proto*-quercitol จึงส่งผลให้ในปฏิกิริยาการปกป้องหมู่ไฮดรอกซิลของสารประกอบชนิดนี้เกิดขึ้นอย่างมีความจำเพาะ ซึ่งจะนำไปสู่การดัดแปลงหมู่ฟังก์ชันที่เหลือจากการปกป้องนี้ เป็นผลิตภัณฑ์เป้าหมาย คือสารประกอบอะมิโนเคอร์ซิทอลได้อย่างสมบูรณ์ด้วยวิธีการที่ไม่ซับซ้อน วิธีการดังกล่าวนี้สามารถใช้เตรียมสารอะมิโนไซคลิทอลในปริมาณที่มากได้ นอกจากนี้ในงานวิจัยนี้ยังได้ศึกษาสเตอริโอเคมีสัมบูรณ์ ของ (+)-*proto*-quercitol เป็นครั้งแรกโดยดัดแปรงจากวิธีของ Mosher สารที่สังเคราะห์ได้ทั้งหมดรวมถึงสาร (+)-*proto*-quercitol ซึ่งเป็นสารตั้งต้น ได้นำไปทดสอบฤทธิ์การยับยั้งเอนไซม์แอลฟากลูโคซิเดสด้วยวิธีคัลเลอริมิตรี พบว่า 5*R*-amino-1,2,3,4-cyclohexanetetrol มีฤทธิ์ยับยั้งเอนไซม์ได้ดีที่สุดด้วยค่า IC_{50} เท่ากับ 12.5 μM ซึ่งจะมีฤทธิ์ยับยั้งเอนไซม์ได้ดีกว่ายารักษาโรคเบาหวาน acarbose ถึง 45 เท่า

ภาควิชา เคมี ลายมือชื่อนิสิต วิศุษฎญา วรวะลัย

สาขาวิชา เคมี ลายมือชื่ออ.ที่ปรึกษาวิทยานิพนธ์หลัก ปรีชา ภูวไพรศิริศาล

ปีการศึกษา 2551 ลายมือชื่ออ.ที่ปรึกษาวิทยานิพนธ์ร่วม สัมฤทธิ์ วัชรสินธุ์

5072597623: MAJOR CHEMISTRY
KEYWORDS: α-GLUCOSIDASE INHIBITORS / AMINOCYCLITOLS / DIABETES

WISUTTAYA WORAWALAI : α-GLUCOSIDASE INHIBITORS FROM AMINOCYCLITOL DERIVATIVES. ADVISOR : ASST. PROF. PREECHA PHUWAPRAISIRISAN, Ph.D., CO-ADVISOR : SUMRIT WACHARASINDHU, Ph.D., 58 pp.

An efficient synthesis of diastereomerically pure 5*S*- and 5*R*-amino-1,2,3,4-cyclohexanetetrols and quercitol derivatives from naturally available (+)-*proto*-quercitol was investigated. Proper stereochemistry of (+)-*proto*-quercitol perfectly set up for regioselective protection of hydroxyl group which was further functionalized into the target aminoquercitols in a straightforward manner. The present approach provided a protocol for preparing aminoquercitol in a large quantity. In addition, the absolute stereochemistry of (+)-*proto*-quercitol was first addressed using modified Mosher's method. All the synthesized compounds including (+)-*proto*-quercitol were tested for α-glucosidase inhibitory activity by colorimetric method. Of synthesized aminocyclitols, 5*R*-amino-1,2,3,4-cyclohexanetetrol potentially inhibited α-glucosidase with IC_{50} value of 12.5 μM, which was 45 times greater than that of standard antidiabetes drug acarbose.

Department : Chemistry Student's Signature : Wisuttaya Worawalai
Field of Study : Chemistry Advisor's Signature : Preecha Phuwaprai sirisa
Academic Year : 2008 Co-Advisor's Signature : SUMRIT WACHARASINDHU

ACKNOWLEDGEMENTS

I wish to express my deep gratitude to my advisor, Assistant Professor Dr. Preecha Phuwapraisirisan and co-advisor, Dr. Sumrit Wacharasindhu for their generous assistance, benevolent guidance and encouragement throughout the course of this research.

I would like to gratefully acknowledge the committees, Associate Professor Dr. Sirirat Kokpol, Assistant Professor Dr. Aroonsiri Shitangkoon and Assistant Professor Dr. Wimolpun Rungprom for their comment, guidance and extending cooperation over my presentation.

I would like to express my gratitude to Natural Products Reseach Unit, Department of Chemistry, Faculty of Science, Chulalongkorn University for providing the chemicals and facilities throughout the course of study.

A deep affectionate gratitude is acknowledged to my family for their understanding, encouragement and support throughout the education course and I special thank to Ms. Kamjira Saisin and Ms. Thanchanok Puksasook for their technical assistance. Moreover, I would like to thank all of my friends in the laboratory for their friendships and help during the course of my graduate research.

Finally, I would like to thank MUA & ADB under the Petroleum & Petrochemical Technology Consortium and CU. Graduate school thesis grant for the financial supports.

CONTENTS

LIST OF TABLE

LIST OF FIGURES

LIST OF SCHEMES

LIST OF ABBREVIATIONS

acetone-d_6	deuterated acetone
brd	broad doublet (NMR)
brs	broad singlet (NMR)
calcd	calculated
^{13}C NMR	carbon-13 nuclear magnetic resonance
$CDCl_3$	deuterated chloroform
CD_3OD	deuterated methanol
COSY	correlated spectroscopy
DMSO- d_6	deuterated dimethyl sulfoxide
DMSO	dimethylsulfoxide
D_2O	deuterium oxide
DMF	*N*,*N*-dimethylformamide
DMAP	4-(dimethylamino)pyridine
DNJ	1-deoxynojirimycin
DM	diabetes mellitus
ddd	doublet of doublet of doublet (NMR)
dt	doublet of triplet (NMR)
d	doublet (NMR)
dd	doublet of doublet (NMR)
2D NMR	two dimensional nuclear magnetic resonance
1D NMR	one dimensional nuclear magnetic resonance
ESIMS	electrospray ionization mass spectrometry
equiv	equivalent (s)
FT-IR	fourier transform infrared spectroscopy
GLUT-4	glucose transporter 4
g	gram (s)
^{1}H NMR	proton nuclear magnetic resonance
HMBC	heteronuclear multiple bond correlation experiment
Hz	hertz
HRESIMS	high resolution electrospray ionization mass spectrum
HIV	human immunodeficiency virus

h	hour (s)
IC_{50}	concentration that required for 50% inhibition in vitro
IR	infrared
IDDM	insulin-dependent diabetes mellitus
J	coupling constant
mg	milligram (s)
mL	milliliter (s)
mmol	millimole (s)
m/z	mass per charge
m	multiplet (NMR)
MsCl	mesyl chloride
MTPACl	α-methoxy-α-(trifluoromethyl)-phenylacetyl chloride
M.W.	molecular weight
M	molar
NIDDM	non-insulin-dependent diabetes mellitus
NOESY	nuclear overhauser enhancement spectroscopy
py	pyridine
PDC	pyridinium dichromate
PNP-G	*p*-nitrophenyl-α-D-glucopyranoside
rt	room temperature
s	singlet (NMR)
TFA	trifluoroacetic acid
THF	tetrahydrofuran
TMS	tetramethylsilane
TsOH	*p*-toluenesulfonic acid
TsCl	*p*-toluenesulfonyl chloride
TLC	thin layer chromatography
U	unit
UV	ultraviolet
δ	chemical shift
δ_C	chemical shift of carbon
δ_H	chemical shift of proton

$\Delta\delta_{SR}$	chemical shift difference between corresponding protons in (*S*)-MTPA and (*R*)-MTPA esters
°C	degree celsius
v_{max}	maximum wave number
µL	microliter (s)
µM	micromolar (s)
% yield	percentage yield
$[\alpha]_D$	specific optical rotation

CHAPTER I

INTRODUCTION

Diabetes mellitus (DM) is a syndrome consisting of metabolic, vascular, and neuropathic components that are interrelated. It is defined as a group of metabolic diseases that are characterized by hyperglycemia resulting from defects in insulin secretion or to resistance of the body's cells to the action of insulin, or to a combination of these [1].

Insulin is a hormone, which is released from the pancreas and controls the amount of glucose in the blood. When the person eats or drinks, food is digested into glucose, which is absorbed into the bloodstream and stimulates the pancreas to produce insulin. Glucose is thus transported into the cells when insulin binds to insulin receptor, which straddles the cell membrane of many cells (Figure 1.1) [2].

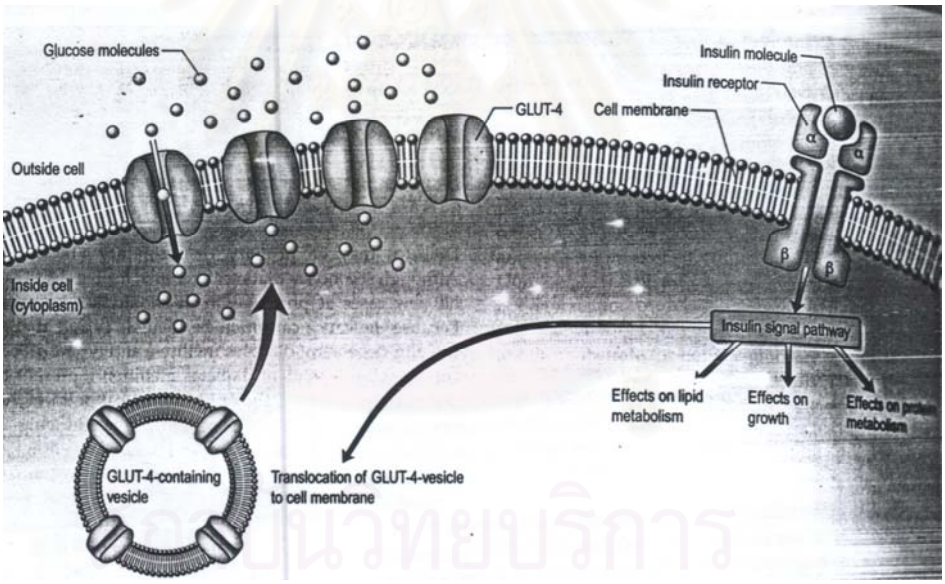

Figure 1.1. Insulin signaling in peripheral cells [4].

The lack of effective insulin action leads to alterations in carbohydrate, fat, and protein metabolism. The chronic hyperglycemia of diabetes is associated with long-term dysfunction and damage of organs including the kidneys, eyes, nerves, heart, and blood vessels. The majority of DM is classified into two categories: type 1 diabetes or insulin-dependent diabetes mellitus (IDDM) and type 2 diabetes or non-insulin-dependent diabetes mellitus (NIDDM), as illustrated in Figure 1.2 [1].

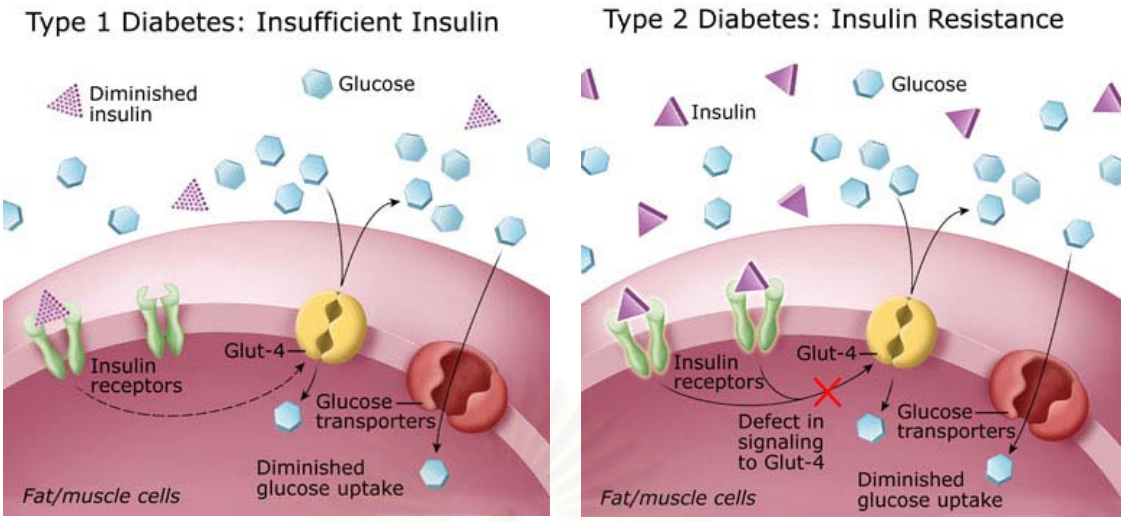

Figure 1.2. Defect from insulin secretion for type 1 DM and insulin resistant for type 2 DM (www.ucsf.mightyminnow.com/images/charts).

Type 1 DM is characterized by loss of the insulin producing of pancreatic β-cell islets, leading to a deficiency of insulin. This type of DM comprises approximately 5% to 10% of all people with DM. It is the most common chronic disease of children and adolescents. The cause of type 1 DM is unknown, but it is believed that people inherit a tendency to develop diabetes, and that viruses may be also involved [2].

Type 2 DM is characterized by insulin resistance or reduced insulin sensitivity, combined with relatively reduced insulin secretion. The defective responsiveness of body tissue to insulin almost certainly involves the insulin receptor in the cell membranes (Figure 1.2). This type of DM comprises approximately 90% to 95% of all diabetes. It usually occurs in adult, in addition to young people. In all probability, the causes of type 2 DM lie in environmental and lifestyle factors. Prominence among these factors is obesity, and approximately 50% to 90% of all patients with type 2 DM are obese. Intraabdominal fat deposition is the important site conveying enhanced risk for type 2 DM. Moreover, other risk factors contain increasing age, high caloric intake, sedentary lifestyle, and low weight [2, 3].

Currently, type 2 DM is increasing in prevalence worldwide and is estimated to affect 200 million people. In Thailand, there are currently over 3 million people with type 2 DM [4, 5]. The main complications of DM include retinopathy, nephropathy, neuropathy, and cardiovascular disease. Thus type 2 DM is a leading cause of blindness, renal failure, amputation, and death from cardiovascular disease.

Treatment of type 2 DM has several approaches that differ at many stages of the condition. In the early stages, many people with type 2 DM can control their blood glucose levels by diet, exercise, and weight loss [5]. Moreover, an efficient therapeutic approach for treatment of type 2 DM is to delay the postprandial hyperglycemia by retarding the rate of carbohydrate digestion through the inhibition of α-glucosidase enzyme [6].

1.1 α-Glucosidase inhibitors

In the small intestine, starch is digested to oligosaccharide by amylase, and further digested by membrane-bound α-glucosidase (isomaltase, maltase, and sucrase) to glucose (Figure 1.3) via the hydrolytic cleavage of α-1,4-glycosidic bond. The mechanism of glycoside cleavage have been reviewed several times recently [7], involving a covalent glycosyl-enzyme intermediate. The detailed mechanism of hydrolysis is demonstrated in Figure 1.4. Generally, α-glucosidase enzyme has two carboxyl groups in the active site that afford the catalysis. Initially, one of the carboxyl groups functions as a general acid catalyst, protonating the glycosidic oxygen simultaneously with bond cleavage. The remaining carboxylate group as a nucleophile, forming a covalent glycosyl-enzyme intermediate. Further, the side-chain carboxylate deprotonates the incoming water molecule, which attacks at the anomeric center and displaces the sugar. This mechanism occur via transition states which involved generating oxocarbenium ion character.

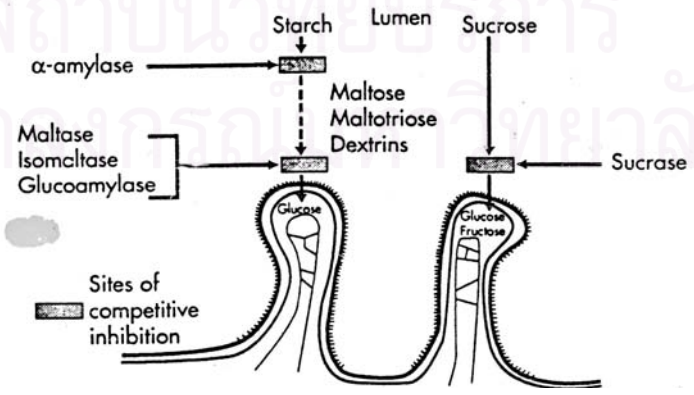

Figure 1.3. Digestion of starch in the small intestine by α-glucosidase enzyme [1].

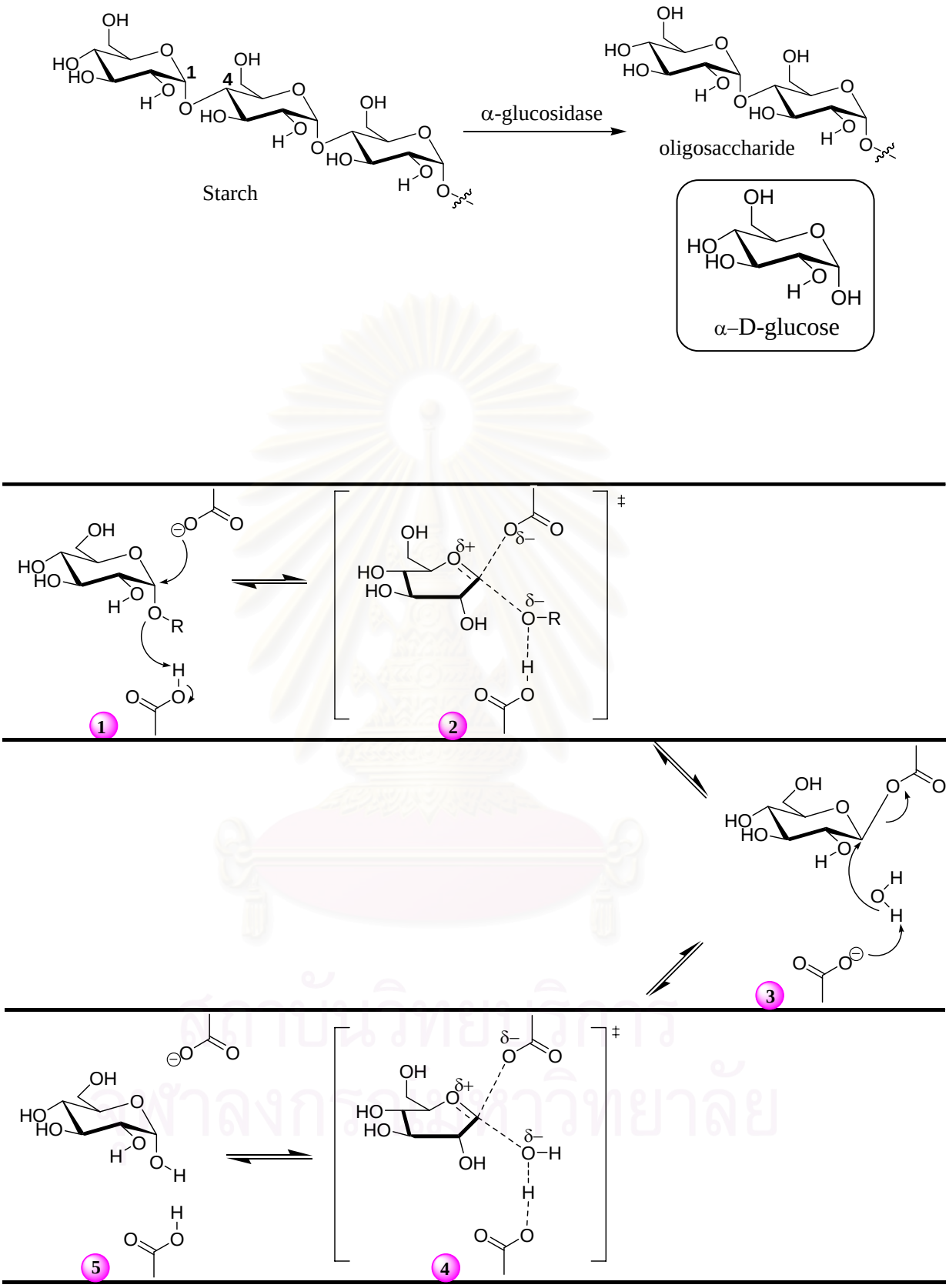

Figure 1.4. Mechanism of enzymatic hydrolysis.

The α-glucosidase inhibitors display their structures as mimic of the oligosaccharide substrate. They competitively bind to the active site of the α-glucosidase, therefore preventing the binding and enzymatic hydrolysis of the oligosaccharide substrate (Figure 1.5). In this way, α-glucosidase inhibition represents a pharmacologic approach for modifying the digestion and absorption of dietary carbohydrates as an adjunct to dietary changes. Because of their competitive mechanism of action, α-glucosidase inhibitors need to be taken at the start of a meal.

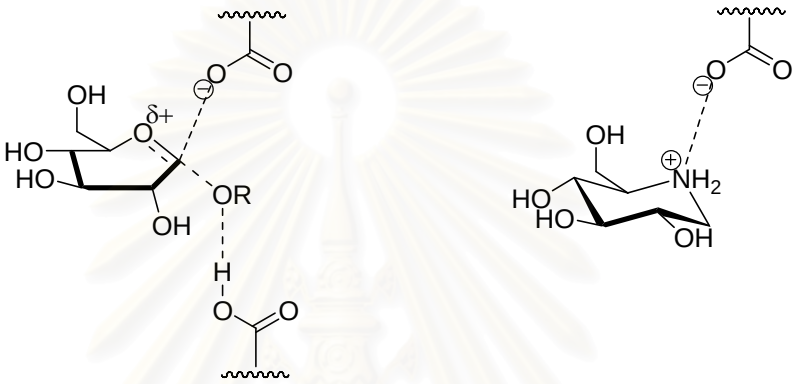

natural substrate: D-glucose DNJ

Figure 1.5. Transition state in reaction of D-glucose with α-glucosidase (left), and inhibitors DNJ (right).

After inhibiting the breakdown of carbohydrate by α-glucosidase inhibitors, in turn causing a reduction in the rate of glucose absorption and also blunting the postprandial plasma glucose level [8]. Moreover, the α-glucosidase inhibitors not only decrease the postprandial increment in plasma insulin level and triglyceride level, but also show antiviral, anticancer and anti-HIV activity [9-11]. Therefore, the α-glucosidase inhibitors are utilized as the oral antidiabetic drugs for example acarbose (Precose® or Glucobay®) (**1**), voglibose (Basen®) (**2**) and miglitol (Glyset®) (**5**) which are recently introduced onto the drug market [12] (Figure 1.6).

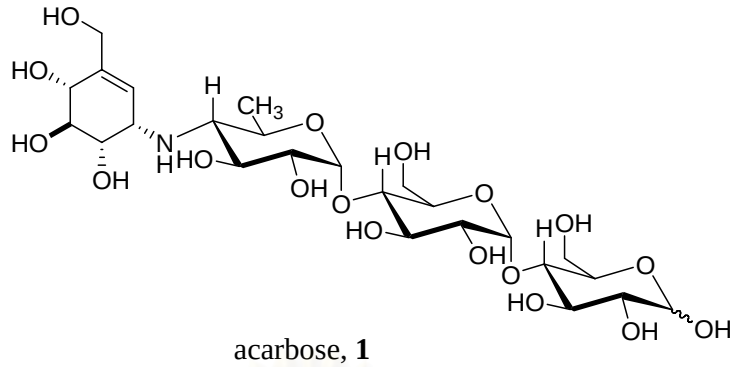

acarbose, **1**

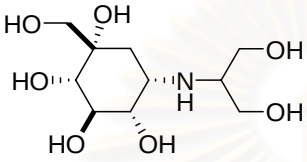

voglibose, **2**

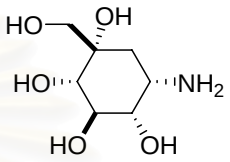

valiolamine, **3**

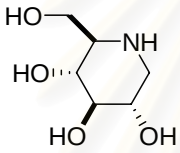

DNJ, **4**

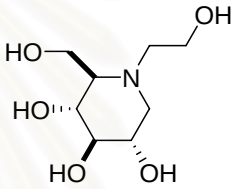

miglitol, **5**

Figure 1.6. Structures of digestive α-glucosidase inhibitors.

Acarbose (Precose® or Glucobay®, **1**) (Figure 1.6), a prominent α-glucosidase inhibitor, was first isolated from soil bacteria *Actinoplanes* sp [13]. Catalytic hydrogenation of acarbose afforded fragments consisting of trisaccharide derivatives. Acarbose was effective in carbohydrate loading tests in rats and healthy volunteer, reducing postprandial blood glucose and increasing insulin secretion [14].

Voglibose (Basen®, **2**), which has a high inhibitory activity against sucrase and maltase, has been employed in Japan for the treatment of diabetes since 1994. It was synthesized from valiolamine (**3**) via reductive amination with dihydroxy acetone. In current studies based on α-glucosidase inhibitory activity [12], it was shown to be 20 to 30 times more potent than acarbose.

In 1996, 1-deoxynojirimycin (DNJ, **4**) was isolated from the roots of mulberry tree [12]. Despite the excellent α-glucosidase inhibitory activity *in vitro*, its efficacy *in vivo* was only moderate. Therefore, a large number of DNJ derivatives were prepared in the expect of increasing the *in vivo* activity. Thus miglitol (Glyset®, **5**)

was discovered as the most favorable inhibitor of *in vivo* active agents which showed reducing postprandial blood glucose level.

Several investigations indicated that oral antidiabetic drugs exerted their activity via competitive binding with α-glucosidase. They are believed to mimic the charge of the presumed transition state for enzymatic glycoside hydrolysis, owing to the protonation of their nitrogen atom in the enzyme active site (Figure 1.5) [3, 9].

To date, over the course of aminocyclitols have been synthesized [15] and their biological activities, particularly glycosidase inhibition, were evaluated. Interestingly, some of them have entered clinical trial or launched in the market.

1.2 Synthesis of aminocyclitol derivatives

Aminocyclitol is broadly defined as a cycloalkane polyol encompassing amino group or incorporating nitrogen atom into the ring. Because of their structures closely similar to sugars, aminocyclitols are also considered as amino-carbasugars [16]. The nitrogen atom in aminocyclitol could be protonated at physiological pH, which mimics the oxocarbenium intermediate formed during enzymatic catalysis (Figure 1.5) [17].

Natural aminocyclitols are abundant as subunits in some complex metabolites, which included acarbose (**1**), validamycin A (**6**) from *Streptomyces hygroscopicus* and validoxylamine A (**7**). However, simple aminocyclitols, such as valienamine (**8**) and validamine (**9**) have also been encountered, presumably as microbial degrades of the complex aminocyclitols [12, 15].

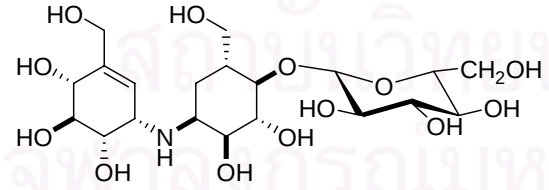

validamycin A, **6**

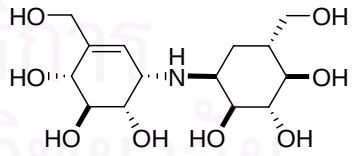

validoxylamine A, **7**

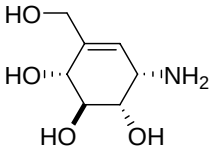

valienamine, **8**

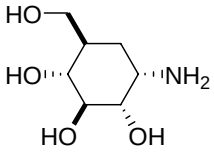

validamine, **9**

Figure 1.7. Aminocyclitols isolated from natural sources.

Recently, the syntheses of aminocyclitols have attracted considerable interest and the synthetic approaches have been developed. A variety of synthetic methodologies for aminocyclitols were described in a current literature [15], in which the key steps involved intramolecular cyclizations, rearrangements, and nucleophilic substitution reactions. From several studies, cyclitols have frequently been used as the starting components instead of ordinary monosaccharides because they provided a shortcut to the target molecules. These have been exemplified by the use of inositol (**10**), quercitol (**11**), conduritol (**12**) and quinic acid (**13**) [18] (Figure 1.8).

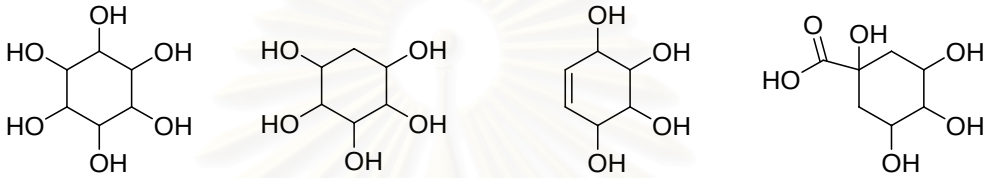

inositol, **10** quercitol, **11** conduritol, **12** quinic acid, **13**

Figure 1.8. Structure of certain natural cyclitols. (Stereochemistry are not shown as each has more than one stereoisomer)

Inositol is a group of cyclitols, in which cyclohexane ring is fully substituted by six hydroxyl groups. It is an attractive chiral pool in synthesis of aminocyclitols possibly due to its capability in generating a variety of products from nine naturally available stereoisomers [19].

In 2007, Arjona *et al*. reported the synthesis of valiolamine from *myo*-Inositol (**14**, Scheme 1.1) [20]. In the initial step, *myo*-inositol (**14**) was transformed into (-)-*vibo*-quercitol (**15**) via biodeoxygenation. Then, **15** was biochemically oxidized by microorganism to furnish **16** in high yield. Treatment of the crude ketone **16** with diazomethane yielded spiro-epoxide **17**, which was subsequently transformed into the 5-hydroxyl derivative **19**. The amino group was introduced to cyclitol moiety via nucleophilic substitution with azide to obtain, after hydrogenolysis and deprotection, (+)-valiolamine (**21**).

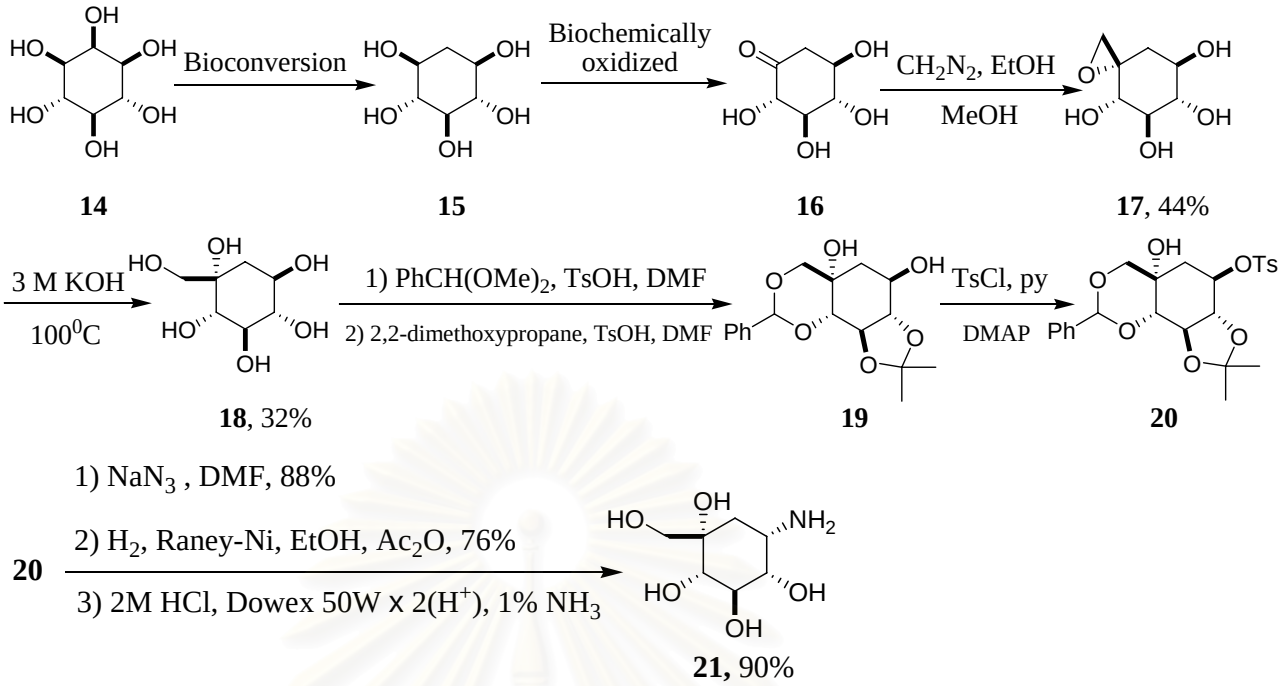

14 **15** **16** **17**, 44%

18, 32% **19** **20**

20 → **21,** 90%

Scheme 1.1. Synthesis of (+)-valiolamine (**21**) from *myo*-inositol (**14**).

Another synthesis of aminocyclitol derivatives using *myo*-inositol was elaborated by Sureshan and co-workers [21]. In the first step, they attempted to protect hydroxyl groups using 2,2-dimethoxypropane, thus giving racemic 1,2:4,5 di-*O*-isopropylidine-*myo*-inositol (±)-**22**. Acylation of (±)-**22** with (*S*)-*O*-acetyl-mandeloyl chloride, as a chiral auxiliary reagent, afforded diastereomeric di-(*S*)-*O*-acetyl-mandelate derivative. This mixture was separated by crystallization, and the chiral auxiliaries were removed by aminolysis, yielding optically active derivatives **25** and **26**. Finally, aminocyclitol **29** was obtained from **26** through azidolysis with sodium azide.

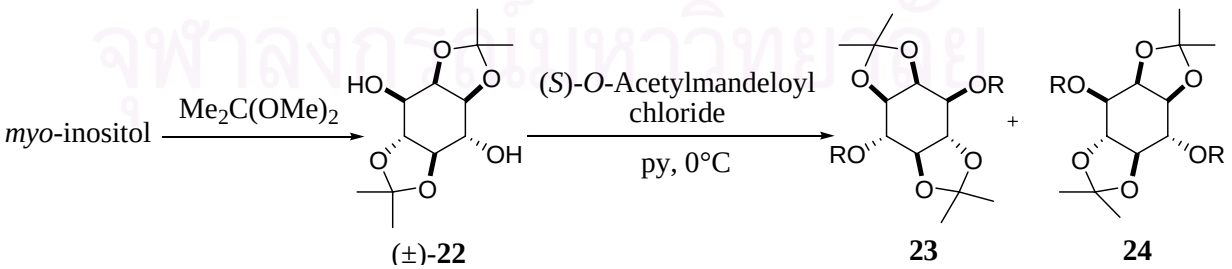

(±)-**22** **23** **24**

R=(*S*)-*O*-acetylmandeloyl

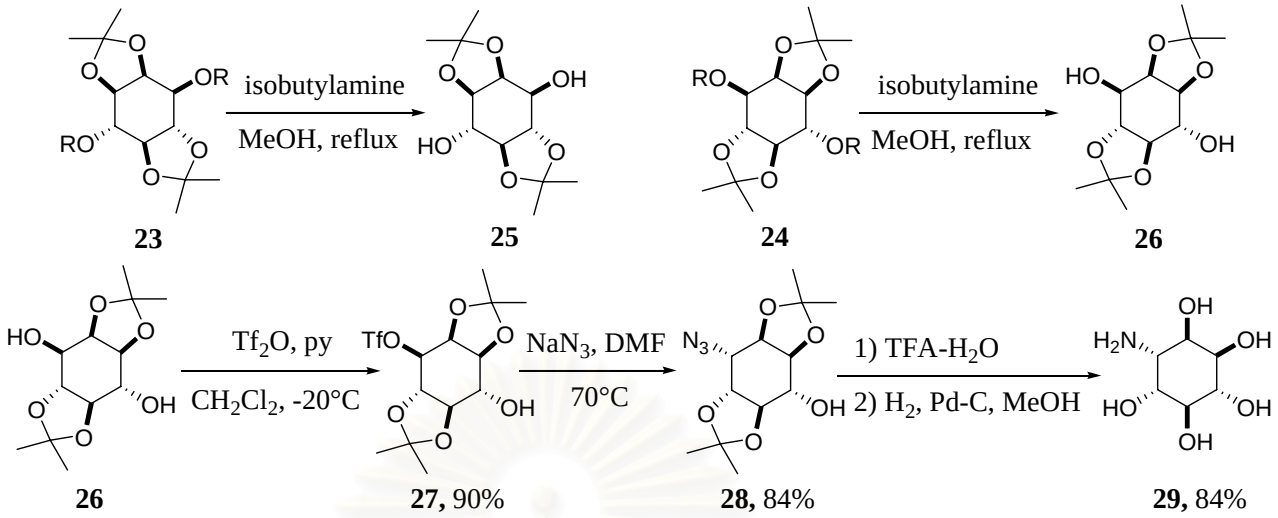

Scheme 1.2. Synthesis of azidocyclitols and aminocyclitols from *myo*-inositol.

On the other hand, conduritols were also used as the starting material for the synthesis of aminocyclitols. The regio- and stereocontrolled epoxide opening of a suitably protected conduritol-B epoxide (**30**) was reported by Gabas and co-workers [22]. Treatment of epoxide **30** with $LiClO_4$ followed by sodium azide gave corresponding C1 regioadduct **31** (Scheme 1.3). This result showed that Li salt promoted epoxide opening via an intramolecular chelation process, which would require the participation of an apparently highly energetic all-axial conformation. Amide analogues **37**-**39** were obtained from azide **32** via reduction, nucleophilic substitution and *O*-benzyl deprotection, respectively. On the other hand, treatment of epoxide **30** with sodium azide under acidic condition (excess NH_4Cl) afforded the corresponding C2 regioadduct **43**. Aminocyclitols **49**-**51** were eventually obtained in good overall yield via reduction of azide **43** followed by reductive amination and *O*-benzyl deprotection (Scheme 1.4).

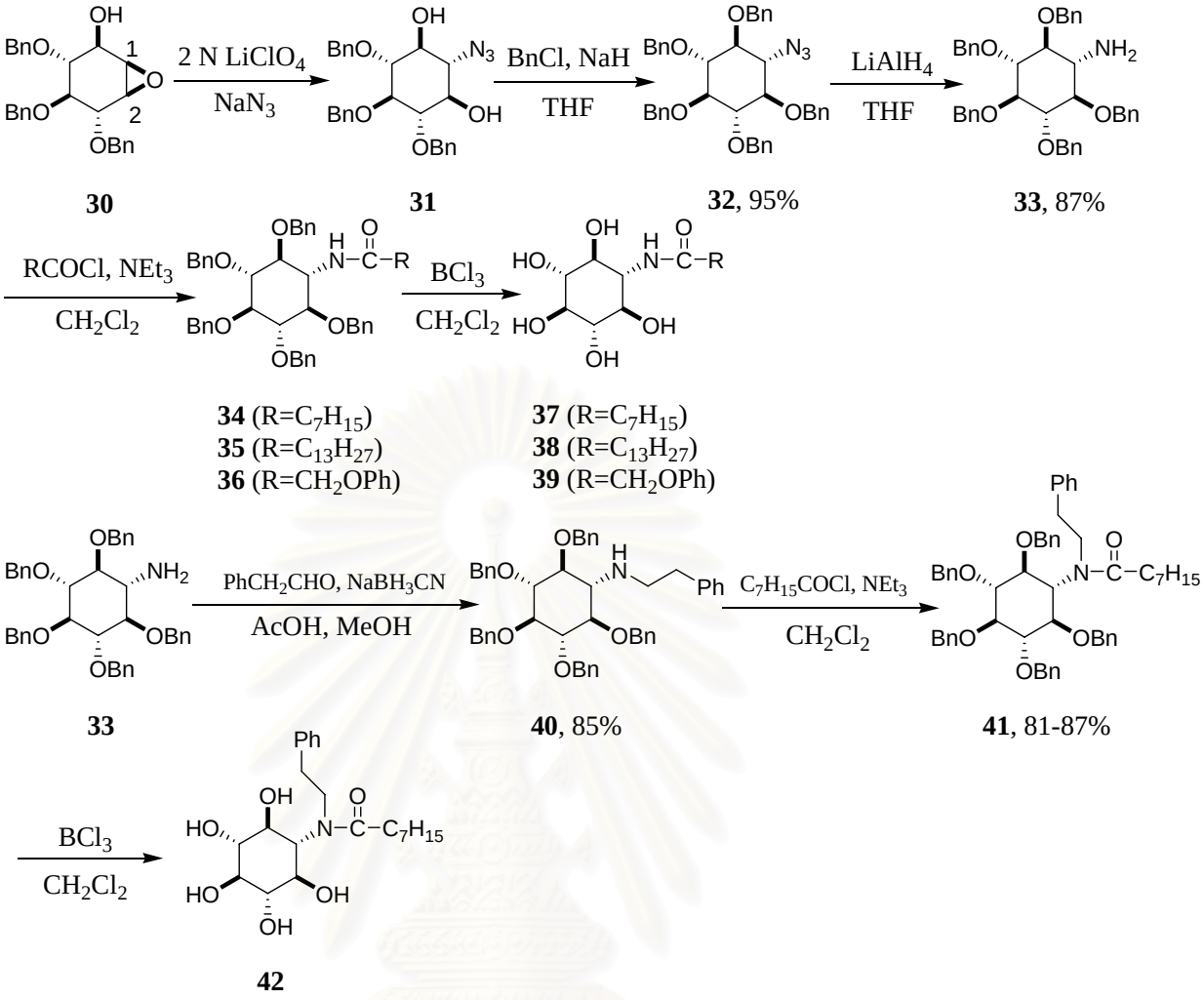

30 **31** **32**, 95% **33**, 87%

34 (R=C_7H_{15}) **37** (R=C_7H_{15})
35 (R=$C_{13}H_{27}$) **38** (R=$C_{13}H_{27}$)
36 (R=CH_2OPh) **39** (R=CH_2OPh)

33 **40**, 85% **41**, 81-87%

42

Scheme 1.3. Synthesis of *N*-acylcyclitols **37-39** and **42** by regioselective C1 opening of epoxide **30**.

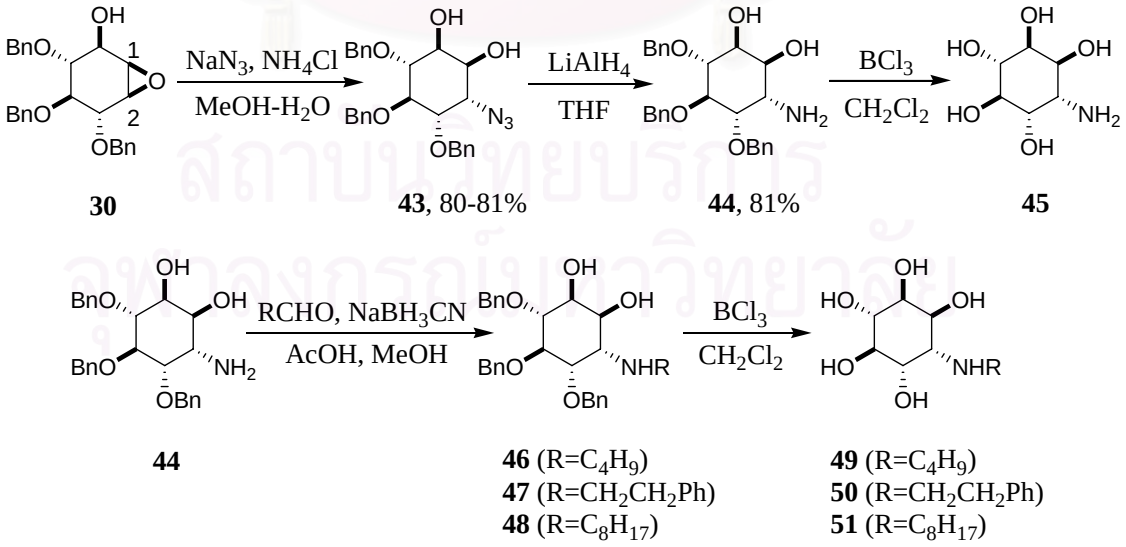

30 **43**, 80-81% **44**, 81% **45**

44

46 (R=C_4H_9) **49** (R=C_4H_9)
47 (R=CH_2CH_2Ph) **50** (R=CH_2CH_2Ph)
48 (R=C_8H_{17}) **51** (R=C_8H_{17})

Scheme 1.4. Synthesis of aminocyclitols **45** and **49-51** by regioselective C2 opening of epoxide **30**.

Quinic acid is one of naturally versatile chiral blocks frequently applied for synthesis of several pharmacological drugs, which include aminocyclitol analogues. Synthesis of valiolamine (**61**) and its diastereomers (**66** and **69**) from (-)-quinic acid (**52**) were reported by Shing and Wan [23]. Valiolamine (**61**) was obtained in 14 steps with a total yield of 8.4% (Scheme 1.5). On the other hand, two diastereomers of valiolamine named 1-*epi*-valiolamine (**66**) and 2-*epi*-valiolamine (**69**) were also prepared from the intermediate **56** in 5 and 4 steps, respectively (Scheme 1.6 and 1.7).

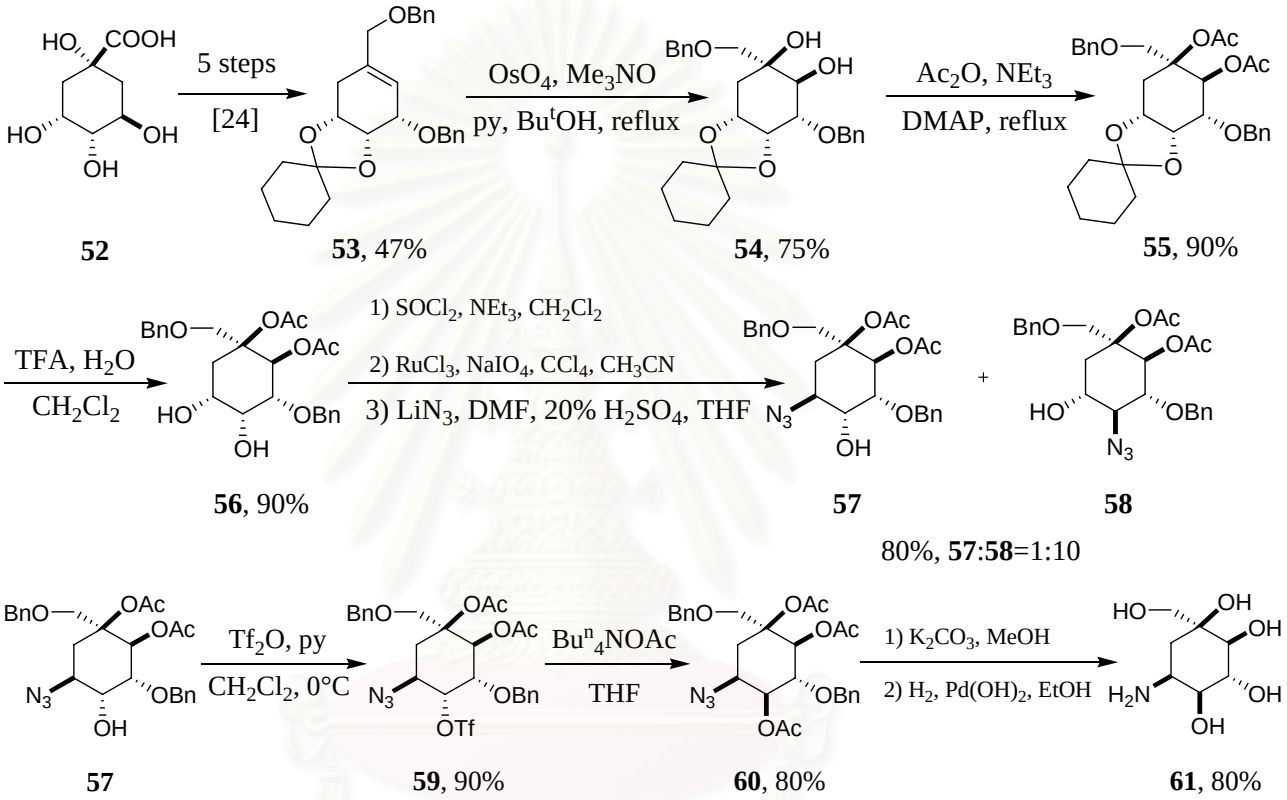

Scheme 1.5. Synthesis of valiolamine (**61**).

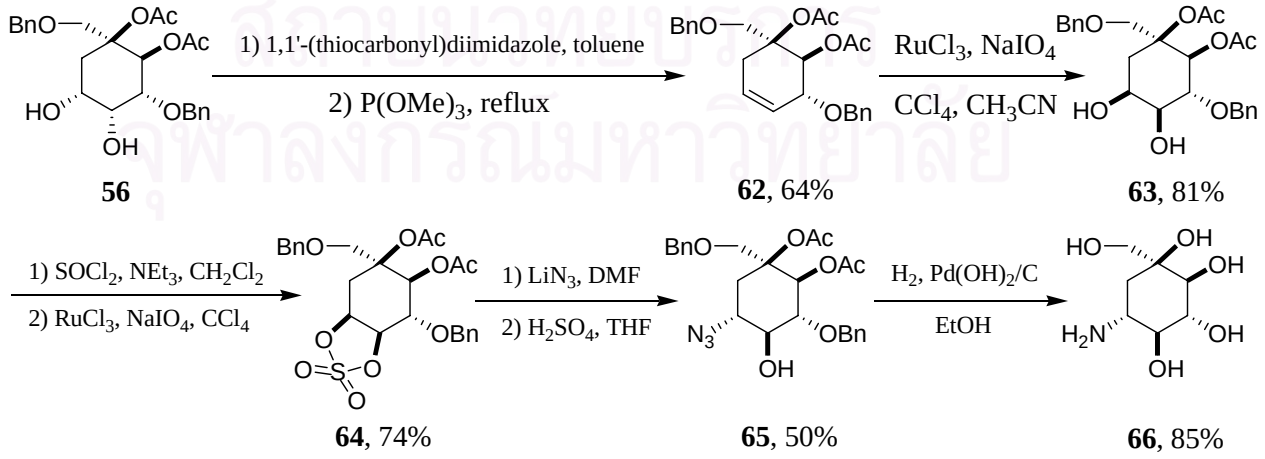

Scheme 1.6. Synthesis of 1-*epi*-valiolamine (**66**).

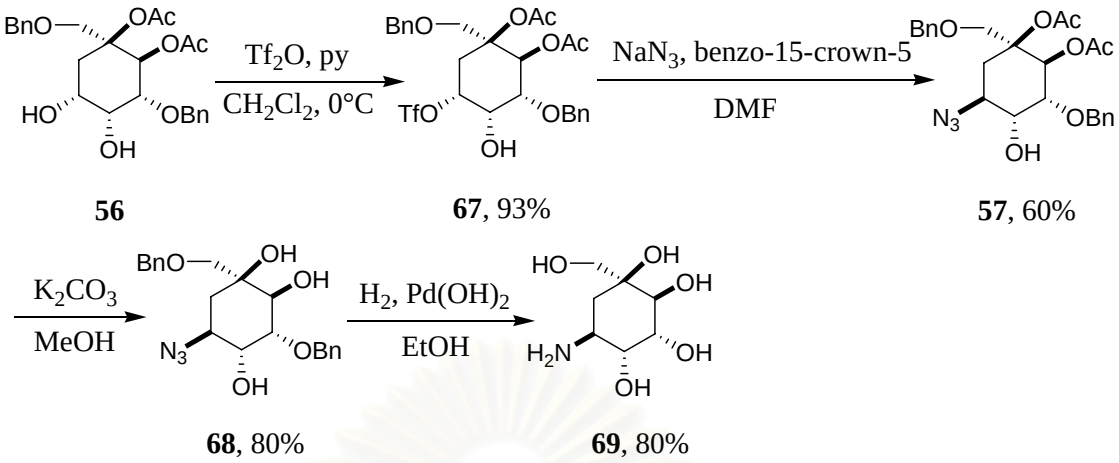

56 **67**, 93% **57**, 60%

68, 80% **69**, 80%

Scheme 1.7. Synthesis of 2-*epi*-valiolamine (**69**).

During the development of the synthesis of an aminocyclitol analog, Kok *et al*. demonstrated new strategy to install effectively the amino group into the polyhydroxycyclohexane skeleton using a regio- and stereospecific palladium-catalyzed reaction [25]. In the report, (-)-quinic acid was used as starting material in the synthesis of valienamine. In early steps, preparation of intermediate **70** was carried out in 13 steps using the similar procedures of a previous literature [26]. Later, alcohol **71** was converted into alkene **72** employing Martin sulfurane dehydrating agent in dry benzene under reflux. The diacetate **72** obtained as a precursor for the syntheses of various *N*-alkylated valienamine derivatives through palladium-catalyzed allylic amination. From this stage, **72** was allowed to react with benzylamine in the presence of a catalytic amount of tetrakis-(triphenylphosphine) palladium [$Pd(PPh_3)_4$] and with triphenylphosphine (PPh_3) in CH_3CN under reflux, affording amine **73** in 65% yield. The valienamine (**75**) was then generated via deprotection as illustrated in Scheme 1.8.

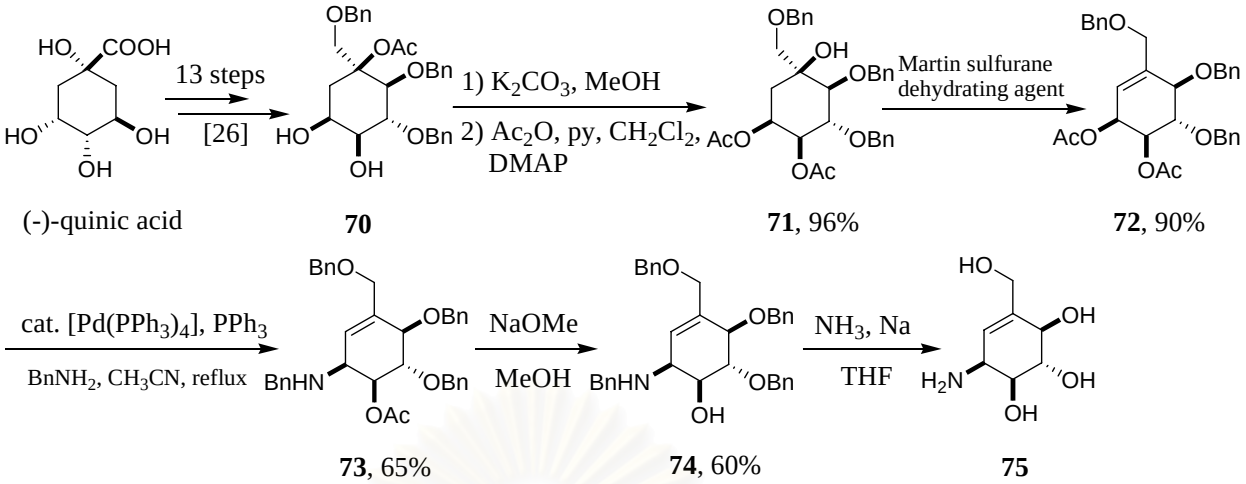

Scheme 1.8. Synthesis of valienamine (**75**) from (-)-quinic acid.

Recently, several syntheses of aminocyclitols have been accomplished using cyclohexanepentols or trivially called quercitols as starting components. In fact, quercitol has 16 possible stereoisomers in its family. Of all isomers, there are only (+)-*proto*-, (-)-*proto*-, and (-)-*vibo*-quercitols being encountered abundantly in nature [27].

The syntheses of aminocyclitols starting from quercitols were described by Ogawa [28, 29]. In 2001, 1-, 2-, and 3-*C*-(amino)-1,2,3,4,5-cyclohexanepentols and *N*-acetyl derivatives were prepared from (+)-*epi*-quercitol. Treatment of **76** with large excess of 2,2-dimethoxypropane gave, after fractionation over a silica gel column, 1,2:3,4-, 1,2:4,5-, and 2,3:4,5-di-*O*-isopropylidine derivatives (**77**-**79**) in 22, 22, and 33% isolated yield, respectively. Later, bisacetonide analogues (**77**-**79**) were separately oxidized with acetic anhydride in DMSO to give the ketone compounds (**80**-**82**) in 91, 70, and 96% yield, respectively. The ketones **80**-**82** were treated with nitromethane to afford moderate yield of nitromethyl-branched derivatives, which were subsequently treated with acetic anhydride in the presence of Raney nickel catalyst to give *N*-acetyl derivatives **83**-**85** in 25, 71, and 63% yield, respectively. Finally, deprotection of **83**-**85** yielded *N*-acetyl aminocyclitols **86**-**88** in 89, 88, and 90% yield, respectively. In addition, aminocyclitols **89**-**91** were also prepared in high yield by treatment of **83**-**85** with 2 M hydrochloric acid [28].

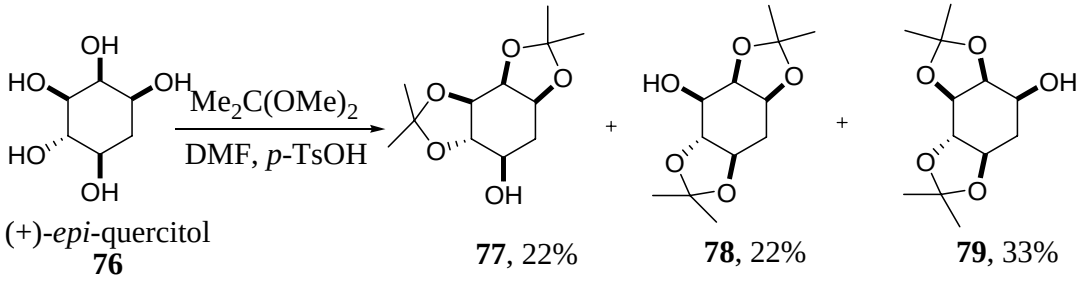

(+)-*epi*-quercitol
76

77, 22% **78**, 22% **79**, 33%

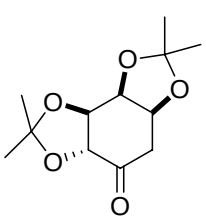

80, 91%

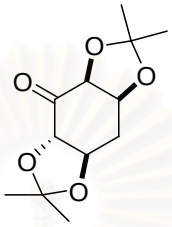

81, 70%

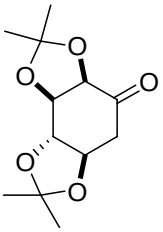

82, 96%

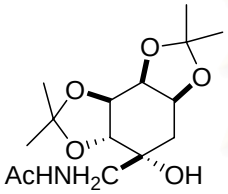

83, 25%

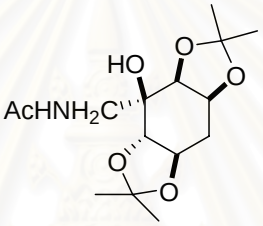

84, 71%

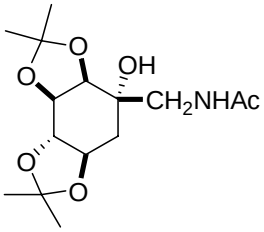

85, 63%

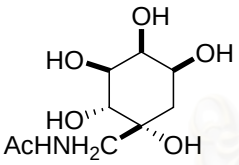

86, 89%

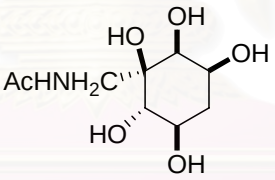

87, 88%

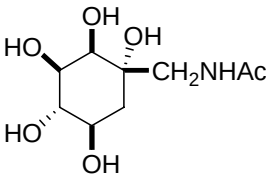

88, 90%

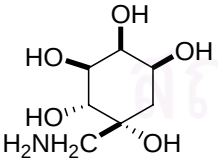

89, 100%

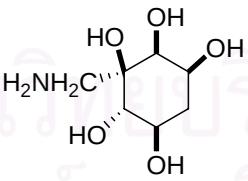

90, 85%

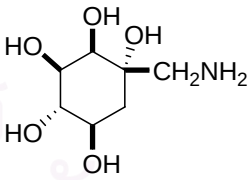

91, 100%

Scheme 1.9. Synthesis of aminocyclitols (**89**-**91**) and *N*-acetyl aminocyclitols (**86**-**88**) from (+)-*epi*-quercitol.

In 2005, 5-amino-1,2,3,4-cyclohexanetetrol derivatives were prepared using (-)-*vibo*-quercitol as the starting material. Protection of **92** with 2,2-dimethoxypropane gave an inseparable mixture of 1,2:3,4- and 1,2:4,5-di-*O*- isopropylidine derivatives (**93** and **94**) in 86% yield. The mixture was treated with sulfuryl chloride in the presence of DMAP in pyridine, giving two chloro compounds **95** (40%) and **96** (58%). Further transformation of **95** into the aminocyclitol **101** involved azidolysis, tosylation, acetolysis, hydrogenation, and deprotection (Scheme 1.10) [29].

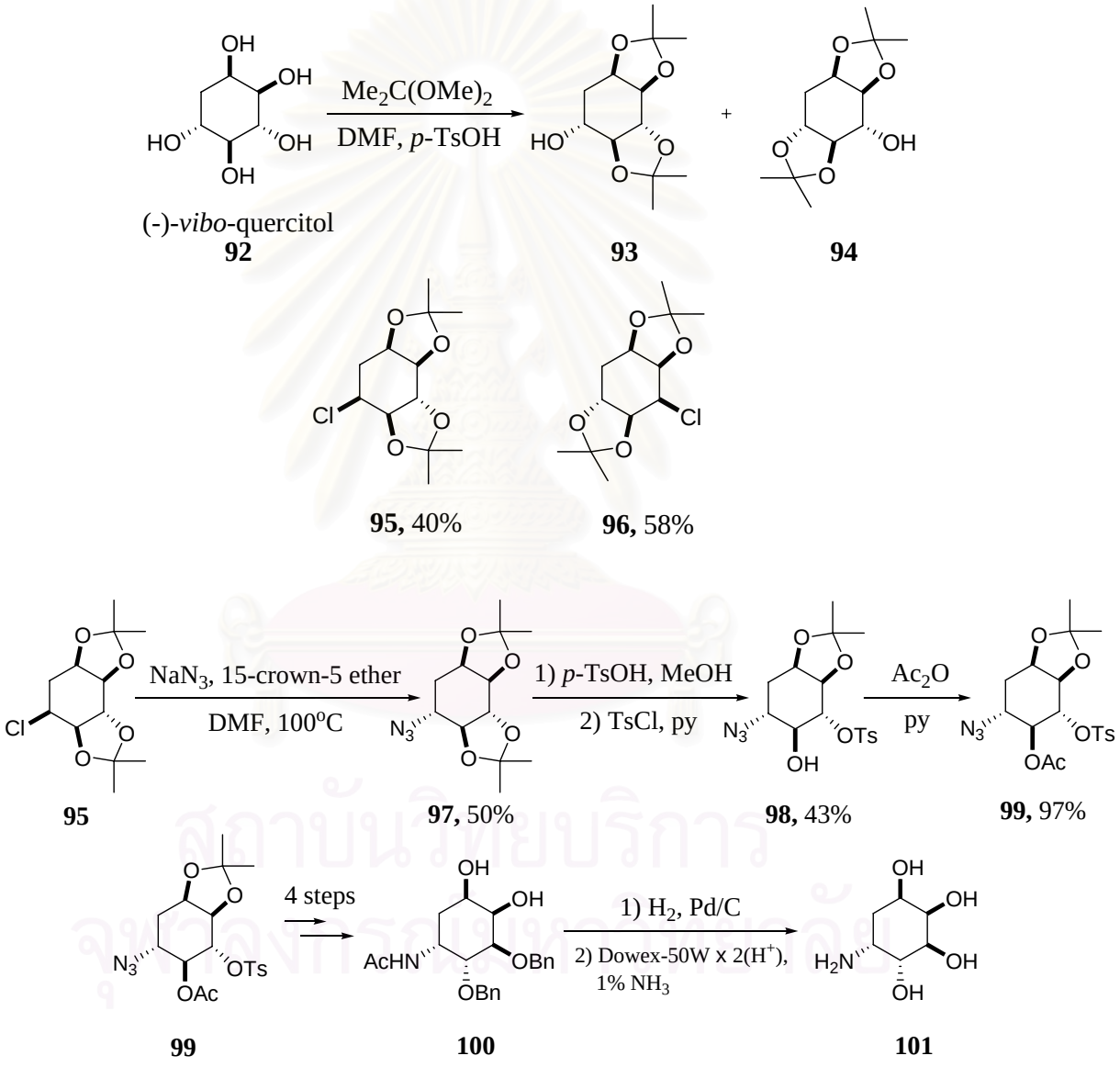

Scheme 1.10. Synthesis of 5-amino-1,2,3,4-cyclohexanetetrol (**101**) from (-)-*vibo*-quercitol.

From the above mention, many research groups reported the preparation of aminocyclitols from the natural carbasugars such as quercitols, conduritols, quinic acid and etc. However, the synthetic procedure required multi-step synthesis and generated unavoidable by-products, resulting in difficult separation and causing lower yield. Thus, in order to reach various families of aminocyclitols displaying various configuration at chiral centers and carrying diverse substituent groups, selection of starting material and excellent synthesis design are crucial.

In this research, we choose (+)-*proto*-quercitol (**102**) as the starting material because there is no report in synthesis of aminocyclitols using this compound. Moreover, (+)-*proto*-quercitol (**102**) could be isolated from *Arfeuillea arborescens* which was first reported in 1998 [30]. Importantly, the isolated (+)-*proto*-quercitol (**102**) is an enantiomeric pure compound and available in large quantities.

With proper configuration of (+)-*proto*-quercitol (**102**), we believe that in the protection of (+)-*proto*-quercitol (**102**) would generate regioselectively single product. Further, the remaining hydroxyl moiety was functionalized into target amino group.

Therefore, the objectives of this research are to synthesize the aminocyclitol derivatives from naturally available (+)-*proto*-quercitol and to determine the α-glucosidase inhibitory activity of the synthesized compounds.

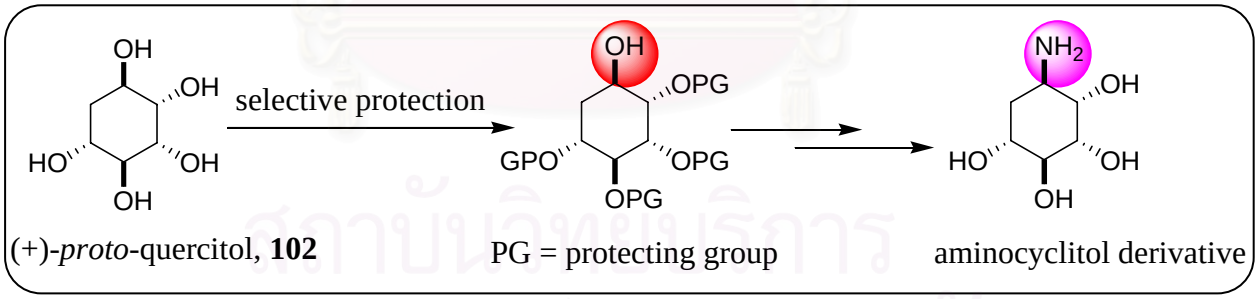

Scope of this research

CHAPTER II

(+)-*proto*-Quercitol, A NATURAL VERSATILE CHIRAL BUILDING BLOCK FOR THE SYNTHESIS OF THE α-GLUCOSIDASE INHIBITORS 5-AMINO-1,2,3,4-CYCLOHEXANETETROLS

2.1. Isolation of (+)-*proto*-quercitol from *Arfeuillea arborescens*

(+)-*proto*-Quercitol (**102**) utilized in this research was isolated from the stems of *Arfeuillea arborescens* using the method previously described with slight modification [30]. Briefly, the MeOH soluble fraction was defatted by partitioning with *n*-hexane. The resulting MeOH soluble part was concentrated under vacuum. After standing the concentrated MeOH soluble part overnight, sugarlike crystal was obtained. It was recrystallized in hot water for several times to obtain pure (+)-*proto*-quercitol. Its structure and relative configuration were characterized by spectroscopic techniques and by comparison with authentic sample. The isolation procedure was summarized in Scheme 2.1.

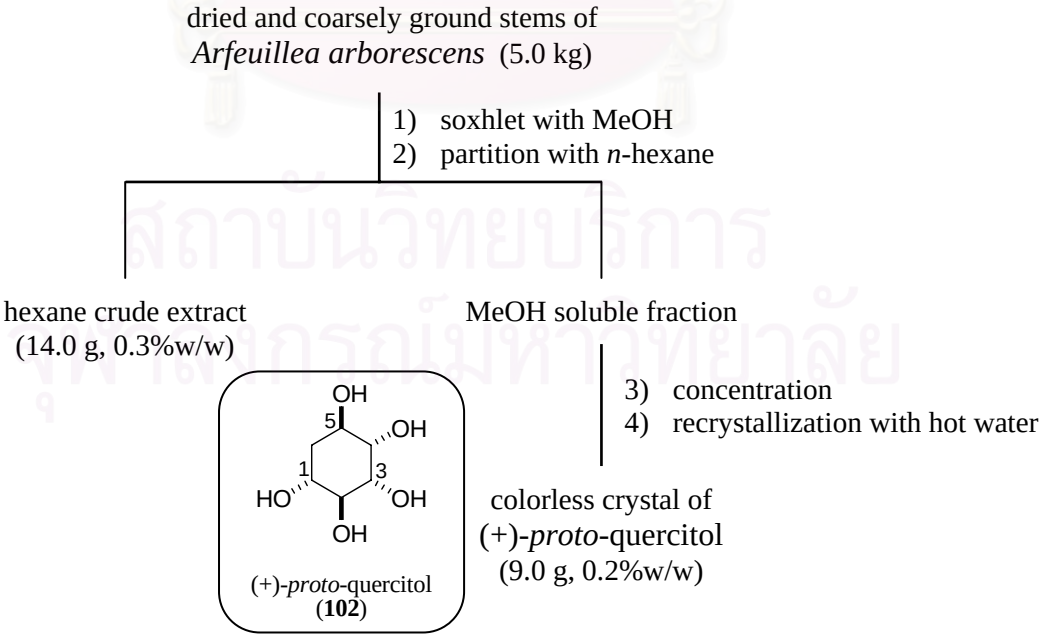

Scheme 2.1. The isolation procedure of (+)-*proto*-quercitol from the stems of *Arfeuillea arborescens.*

2.2. Structural characterization of (+)-*proto*-quercitol

(+)-*proto*-Quercitol was isolated as a colorless crystal, mp 235-236 °C, $[\alpha]_D^{27}$ +27.9 (*c* 0.02, H_2O), from the MeOH soluble fraction of the stems of *A. arborescens.* The molecular formula was determined to be $C_6H_{12}O_5$ (M.W. 164) on the basis of ESIMS. The ^1H NMR data of **102** in D_2O indicated the presence of two proton types, methine and methylene protons. Five downfield signals from δ 3.44 to 3.90 were assigned as methine protons (H-1 to H-5) and two upfield signals from the chemical shifts at δ 1.86 and 1.69 were also assigned as methylene protons (H-6). The ^{13}C NMR spectrum displayed six signals, five of which (δ_C 74.2, 71.8, 70.6, 68.5 and 68.2) were assignable to methine carbons and the remaining signal (δ_C 32.9) was designed to methylene carbon. From the results of MS and 1D NMR data, the structure of compound **102** could be confirmed as (+)-*proto*-quercitol**,** which was completely characterized by 2D NMR data [30].

Although the structure of **102** was established, its absolute configuration has not been addressed. Thus, in this research, we reported the first determination of absolute stereochemistry of **102** using modified Mosher's method [31]. Prior to applying this approach, protection of four hydroxyl groups was required to avoid combined anisotropy effects caused by multiple MTPA moieties [32]. Generally, treatment of **102** with 2,2-dimethoxypropane lead to three possible structures (Scheme 2.2). In fact, from this result, protection of **102** with large excess of 2,2-dimethoxypropane in DMF at 80 °C yielded 1,2:3,4-di-*O*-isopropylidene derivative (**103**) as a single product in 75% yield, without detection of **104** and **105** (Scheme 2.3). The molecular formula of **103** was determined to be $C_{12}H_{20}O_5$ (M.W. 244) on the basis of ESIMS.

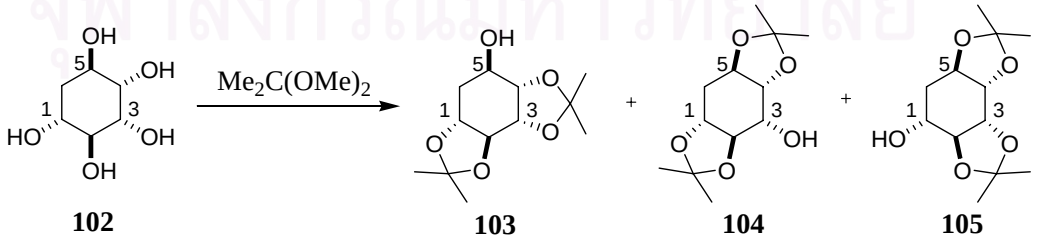

102 **103** **104** **105**

Scheme 2.2. Possible structures of bis-acetonide derivatives (**103**, **104** and **105**) from reaction of **102** with $Me_2C(OMe)_2$.

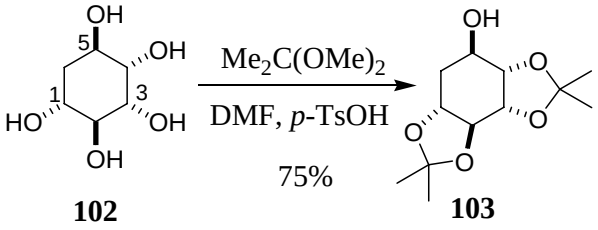

102 **103**

Scheme 2.3. Preparation of 1,2:3,4-di-*O*-isopropylidene derivative (**103**).

The structure and relative configuration of **103** were elucidated using the data of COSY, HMBC and NOESY experiments. The COSY data was used to assign chemical shifts of each signal in cyclohexane ring system. Starting from methylene proton (H-6) at δ 1.95-2.05 (2H, m), the protons showed $^{3}J_{H,H}$ correlations were assigned to H-1 and H-5. Therefore, the remaining signals could be further assigned on the basis of three bond correlation. Prior to establishing relative configuration of quercitol, all methyl groups of bis-acetonide were assigned by HMBC data (Figure 2.1). The NOESY correlations (Figure 2.2) indicated that acetonides formed between C-1 and C-2 and between C-3 and C-4 were *trans*- and *cis*-oriented, respectively. From all above data, the structure of **103** was completely confirmed. In the next step, the bis-acetonide **103** was then treated with (*R*)-(-)- and (*S*)-(+)-MTPACl (Scheme 2.4) separately to furnish the desired (*S*)-(-)- and (*R*)-(+)-MTPA esters (**103a** and **103b**). The $\Delta\delta_{SR}$ distribution pointed out the 5*R* configuration, therefore addressing absolute configurations of remaining chiral centers as shown in Figure 2.3.

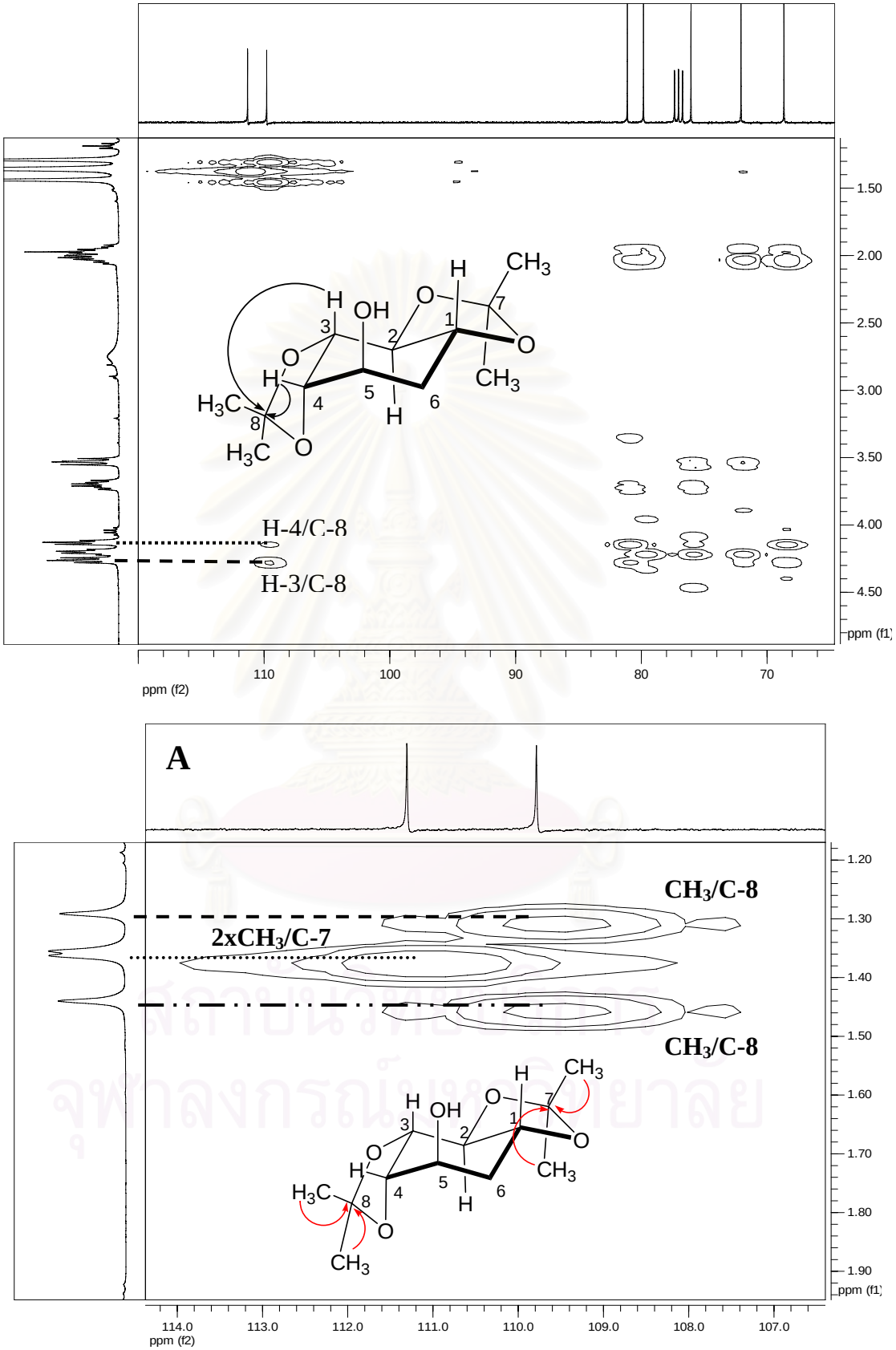

Figure 2.1. Diagnostic HMBC correlations observed in **103**. Expansion (A) shows cross peaks of CH_3 to C-7 and C-8.

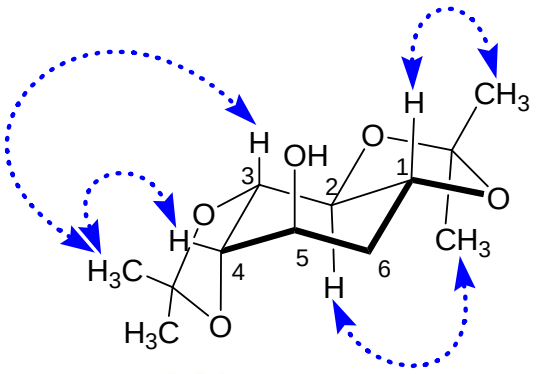

Figure 2.2. Selected NOESY correlations of **103**. For clarity, certain H atoms are omitted.

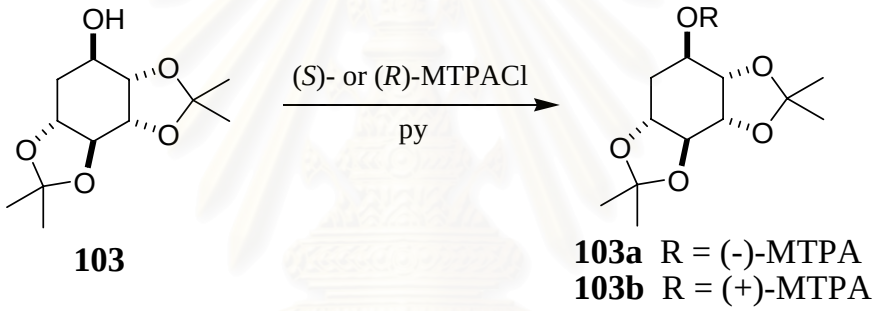

Scheme 2.4. Preparation of **103a** and **103b**.

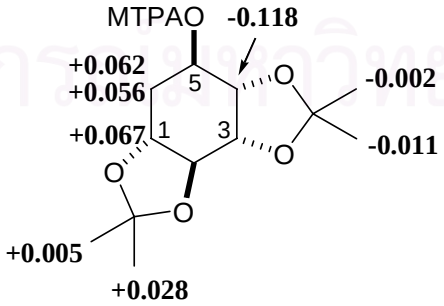

Figure 2.3. $\Delta\delta_{SR}$ Values for the MTPA esters (**103a** and **103b**) of **103**.

2.3. Synthesis of 5-amino-1,2,3,4-cyclohexanetetrols

After the absolute stereochemistry of **103** was established**,** the synthesis of 5*S*-amino-1,2,3,4-cyclohexanetetrol (**111**) was launched. The first attempt to synthesis of chloride **106** using thionyl chloride (3 equiv) in the presence of DMAP in pyridine as solvent was failed. The starting material, alcohol (**103**) was recovered in moderate yield. However, it might be noted that this approach has been succeeded by Ogawa *et al*. [29]. This result can be rationalized in term of steric hindrance from two adjacent acetonide groups which prohibit the attacking of chloride anion (Figure 2.4). Additionally, conversion of acetonide **103** to the corresponding tosylate **107** using *p*-toluenesulfonyl chloride (TsCl) was also unsuccessful; only starting material was recovered.

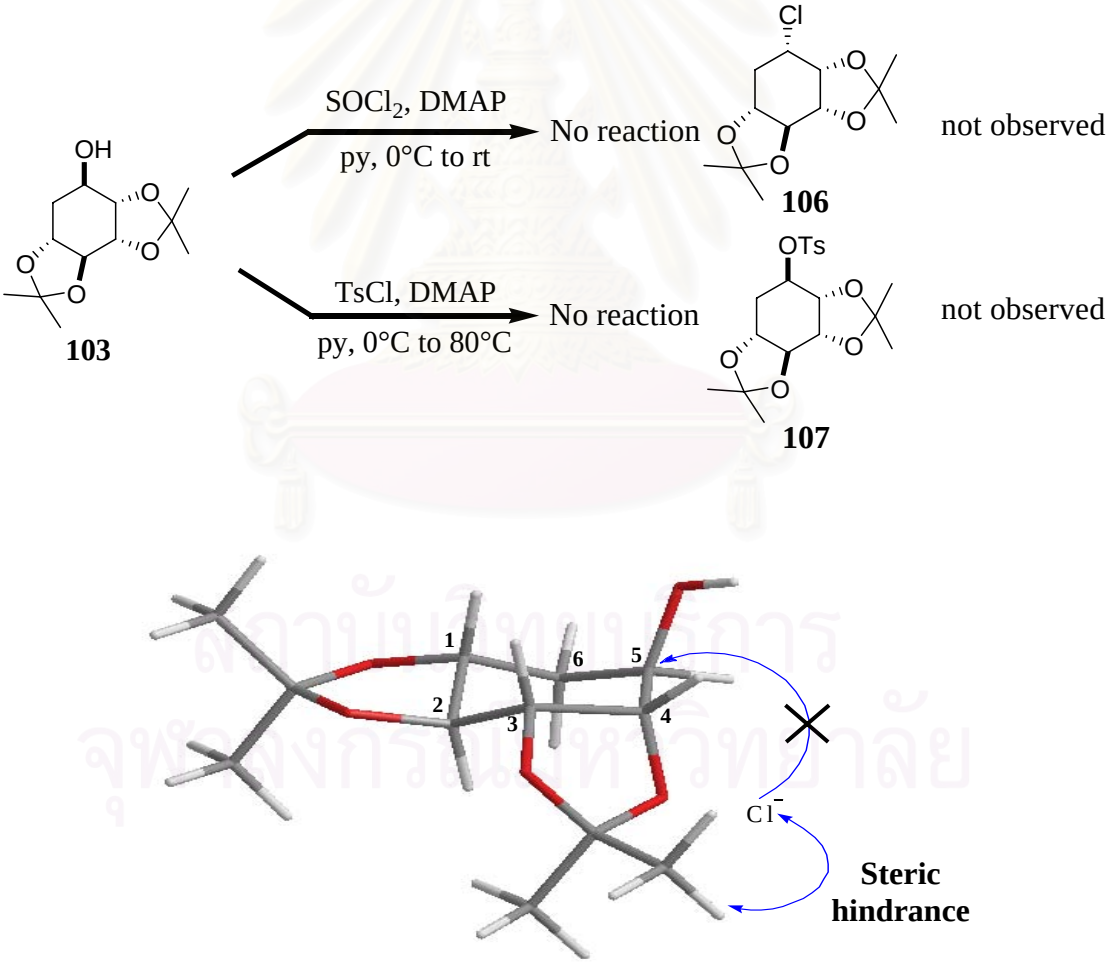

Figure 2.4. Steric effect from acetonide groups for the chlorination of **103**.

From the above result, we need an alternative method to activate hydroxyl moiety of acetonide **103**. Instead of using TsCl, we decided to use a smaller and more reactive reagent, mesyl chloride (MsCl). Treatment of alcohol substrate **103** with this reagent in the presence of DMAP yielded the mesyl analogue (**108**) smoothly (Scheme 2.5). The ^{1}H NMR spectrum of **108** showed obvious separation compared with **103**, the starting material of this reaction. In addition, the most downfield signal at δ_H 5.03 was assigned as H-5 which is adjacent with the mesyl group and the signal of methyl from mesyl group appeared at δ_H 3.07.

With the **108** in hands, the synthesis of target aminocyclitol **111** was accomplished in a straight forward manner as illustrated in Scheme 2.5. Azidolysis of **108** with an excess of sodium azide in DMF at 100 °C in the presence of 15-crown 5-ether afforded selectively the azide **109** (79%) as a sole product after flash chromatography. Interestingly, upon treatment with sodium azide without the introduction of 15-crown 5-ether gave the similar result (74% yield). Therefore, 15-crown 5-ether reagent has no effect in this transformation. The chemical shift at δ_H 3.30 with a large coupling constant ($J_{4eq,5ax}$ = 10.6 Hz) suggested that the azido group was incorporated through a direct S_N2 fashion with inversion of configuration. Furthermore, the IR spectrum of **109** showed a very strong and sharp absorption at ν_{max} 2100 cm^{-1} was also indicated as azido group. In the next reaction sequence, reduction of azide **109** proceeded smoothly upon treatment of $LiAlH_4$, leading to the formation of corresponding amine **110** in 71% yield. In the final step, treatment of amine **110** with trifluoroacetic acid (TFA) in THF at room temperature furnished the target molecule, 5*S*-amino-1,2,3,4-cyclohexanetetrol (**111**) in 63% yield. The ^{1}H NMR spectrum of which fully supported the assigned structure. Particularly, the signals at δ_H 1.27-1.41 disappeared, indicated that the protecting group of **110** was removed by TFA.

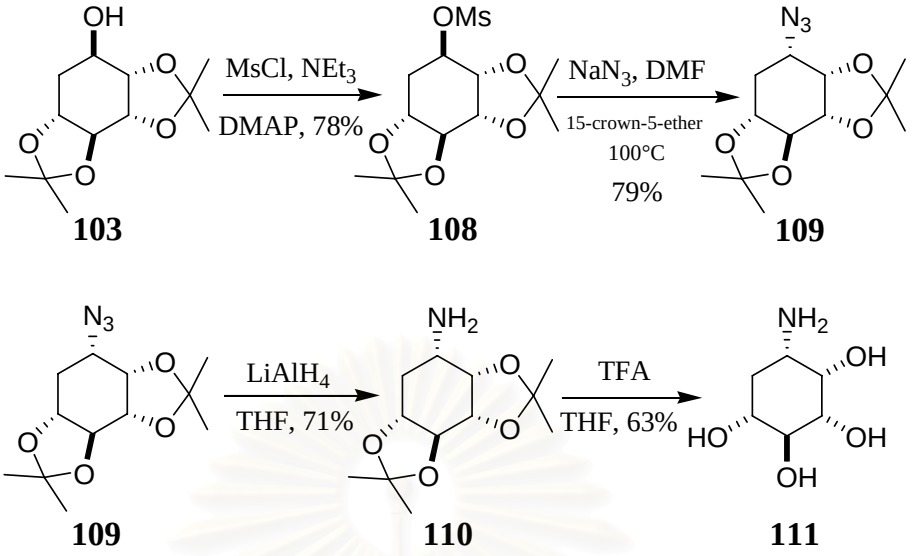

Scheme 2.5. Synthesis of 5*S*-amino-1,2,3,4-cyclohexanetetrol (**111**) from bis-acetonide **103**.

To gain insight into the relationship between stereochemistry of 5-amino group and inhibitory effect toward α-glucosidase, 5*R*-amino congener **117** was also prepared. Initially, oxidation of bis-acetonide **103** with pyridinium dichromate (PDC) in CH_2Cl_2 gave the ketone in low yield (7%) (Scheme 2.6). Later, we tried to improve the yield using Swern oxidation reaction (Scheme 2.6). Unfortunately, this was also unsuccessful. The desired ketone **112** was isolated in small amout. We suspected that the staring material was decomposed under the reaction condition presumably due to acidity from the oxidizing agent. Finally, the bis-acetonide **103** was subjected to oxidation reaction using Albright-Goldman reagent (Ac_2O/DMSO) [33], affording the desired ketone **112** in 55%.

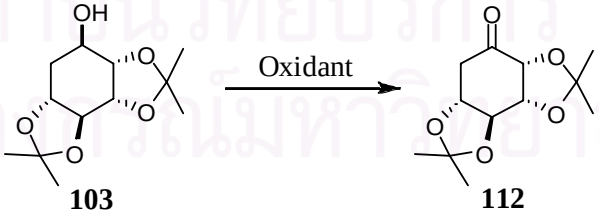

Oxidant	Yield of **112** (%)
(Swern oxidation) $(COCl)_2$, DMSO	No reaction
PDC	7
Ac_2O, DMSO	55

Scheme 2.6. Oxidation of bis-acetonide **103**.

Selective reduction of **112** was carried out with $LiAlH_4$ in THF as a solvent, and diastereomeric 5-hydroxy-bis-acetonide **113** (93%) was isolated without any detection of analogue **103**. This could be rationalized by the preferential hydride attack to the less hindered face of ketone **112.** Obviously, compounds **103** and **113** could be differentiated by ^1H NMR spectra (Figure 2.5); H_2-6 of the former aggregately resonated about δ_H 2.04-2.11 while those of the latter were well separated [δ_H 2.36 ($H\text{-}6_{eq}$) and 1.88 ($H\text{-}6_{ax}$)].

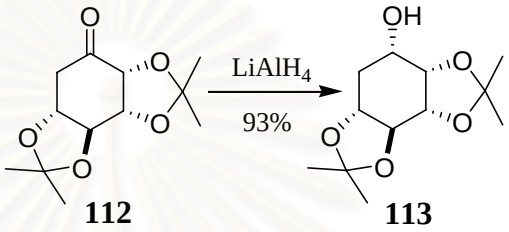

Scheme 2.7. Reduction of ketone **112**.

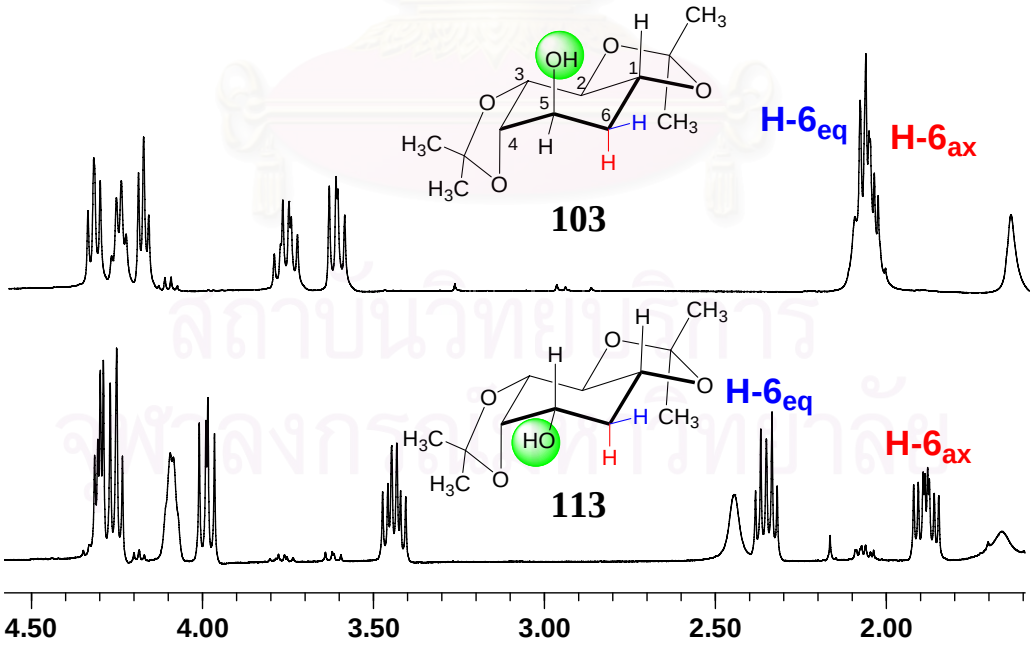

Figure 2.5. Partial ^1H NMR spectra of **103** (top) and **113** (bottom).

With these exciting results, we therefore have the opportunity to prepare the new derivative of aminocyclitol **117**. The synthesis of 5*R*-amino congener **117** was accomplished through similar manner as aminocyclitol **111** starting from the alcohol **113** (Scheme 2.8). Mesylation of alcohol followed by azylation gave rise to the formation of azide **115** in an excellent yield (84% for two steps). The azide **115** was then allowed to react with lithium aluminum hydride and the amine **116** was isolated. To finish the synthesis of aminocyclitol **117**, the amine **116** was exposed to TFA in THF as solvent generated the target aminocyclitol **117** in 86%.

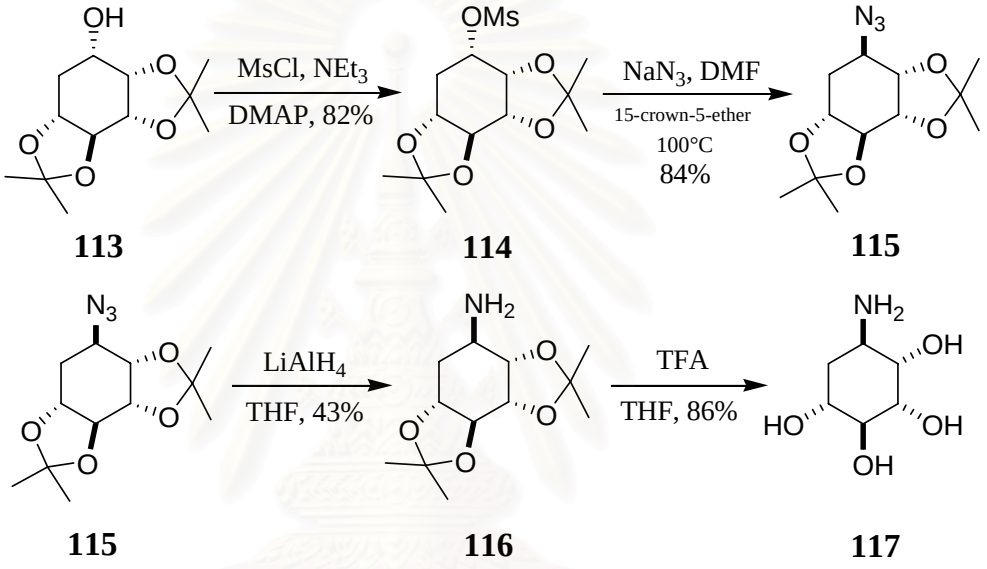

Scheme 2.8. Synthesis of 5*R*-amino-1,2,3,4-cyclohexanetetrol (**117**) from bis-acetonide **113**.

In order to gain more information on the pharmacophore required for C-5, we prepared other cyclitol derivatives. Cleavage of bis-acetonide protecting groups of compound **112** and 1**13** were carried out under the aforementioned conditions. The crude products were purified by recrystallization with hexane afforded pure target cyclitols **118** and **119** in reasonable yields (Scheme 2.9).

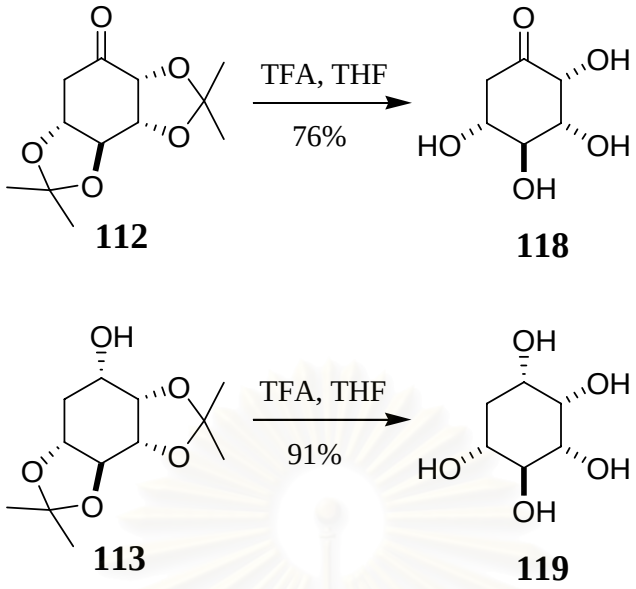

Scheme 2.9. Preparation of **118** and **119**.

2.4. α-Glucosidase inhibitory effect

5-Amino-1,2,3,4-cyclohexanetetrols (**111** and **117**) and deprotected analogues (**118** and **119**) were evaluated for α-glucosidase inhibitory effect using colorimetric method [34] with slight modification. In brief, α-glucosidase hydrolyzed the substrate *p*-nitrophenyl-α-D-glucopyranoside (PNP-G) to produce *p*-nitrophenol and glucose (Scheme 2.10). Therefore, the inhibitory effect of synthesized compounds towards α-glucosidase was quantified by UV (405 nm), in term of *p*-nitrophenol decline.

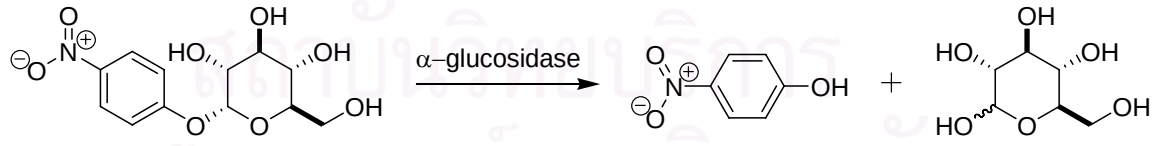

Scheme 2.10. Hydrolysis of α-glucosidase.

The synthesized compounds were tested for the α-glucosidase inhibitory activity, and the results are shown in Table 2.1. All of the synthesized compounds showed weak inhibitory effect (IC_{50} 670-2890 μM) compared with antidiabetes drugs (Acarbose® and DNJ), except for amino cyclitol **117** (IC_{50} 12.5 μM). A tremendous

difference in inhibitory effect of two diastereomeric aminocyclitols **111** and **117** (IC_{50} 2890 vs 12.5 μM) suggested that the configuration of 5-NH_2 was possibly essential for mimicking the conformation and charge of the oxycarbenium ion intermediate [7].

Table 2.1. α-Glucosidase[a] inhibitory effect of compounds **102**, **111**, **117**, **118** and **119**

Compound	Inhibitory effect (IC_{50}, μM)
102	NI[b]
111	2890
117	12.5
118	670
119	921
Acarbose®	570
DNJ	173

[a]α-Glucosidase was obtained from baker yeast. [b]Inhibitory effect less than 30% at 10 mg/mL.

2.5. Experimental section

2.5.1 General experiment procedures

NMR spectra were recorded with a Varian Mercury$^+$ 400 NMR spectrometer operated at 400 MHz for ^1H and 100 MHz for ^{13}C nuclei and JEOL JNM-A500 FT NMR spectrometer operated at 500 MHz for ^1H and 125 MHz for ^{13}C nuclei. The chemical shift in δ (ppm) was assigned with reference to the signal from the residual protons in deuterated solvents and using TMS as an internal standard in some cases. The IR spectrum was recorded on a Perkin-Elmer FT-IR spectroscopy spectrum RXI spectrometer (Perkin Elmer Instruments LLC., Shelton., U.S.A.). ESIMS and HRESIMS were obtained from mass spectrometer model VG TRIO 2000 and a Micromass LCT mass spectrometer, respectively. Silica gel 60 Merck cat. No. 7734 was used for open column chromatography. Thin layer chromatography (TLC) was performed on precoated Merck silica gel 60 F_{254} plates (0.25 mm thick layer).

2.5.2 Plant material

The stems of *Arfeuillea arborescens* were purchased from Chao-Krom-Per, a Thai medical plant shop, Bangkok, Thailand, in October, 2007.

2.5.3 Isolation procedure

Dried and coarsely ground stems of *Arfeuillea arborescens* (5.0 kg) were extracted with MeOH in Soxhlet extractor to yield MeOH soluble fraction which was defatted by partitioning with *n*-hexane (3 × 500 mL). The MeOH soluble part was evaporated in vacuum to give the concentrated one. After standing the concentrated MeOH soluble part overnight, sugarlike crystal was obtained. It was recrystallized in hot water for several times to obtained pure (+)-*proto*-quercitol (9.0 g, 0.2 % w/w).

(+)-*proto*-Quercitol (102)

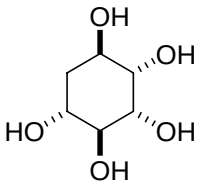

Colorless crystal; mp 235-236 °C; $[\alpha]_D^{27}$ +27.9 (*c* 0.02, H_2O); ^{1}H NMR (DMSO-d_6, 500 MHz) δ 4.66 (d, *J* = 3.4 Hz, OH), 4.49 (d, *J* = 3.7 Hz, OH), 4.42 (d, *J* = 4.3 Hz, OH), 4.37 (d, *J* = 4.9 Hz, OH), 4.26 (d, *J* = 6.1 Hz, OH), 3.67 (ddd, *J* = 7.0, 6.7, 3.7 Hz, 1H), 3.59 (dd, *J* = 3.7, 3.3 Hz, 1H), 3.40-3.51 (m, 2H), 3.28 (dt, *J* = 12.8, 4.0 Hz, 1H), 1.56-1.66 (m, 2H); ^{13}C NMR (DMSO-d_6, 125 MHz) δ 75.0, 72.9, 71.4, 68.9, 68.4. 34.9; ^{1}H NMR (D_2O, 400 MHz) δ 3.90 (dd, *J* = 6.4, 3.2 Hz, 1H), 3.80 (dd, *J* = 3.2, 2.4 Hz, 1H), 3.57-3.66 (m, 2H), 3.44 (dd, *J* = 9.6, 9.2 Hz, 1H), 1.86 (ddd, *J* = 13.9, 3.2, 3.2 Hz, 1H), 1.69 (ddd, *J* = 13.9, 11.6, 2.8 Hz, 1H); ^{13}C NMR (D_2O + one drop acetone-d_6, 100 MHz) δ 74.2, 71.8, 70.6, 68.5, 68.2, 32.9; ESIMS *m/z* $[M+H]^+$ 165.

2.5.4 Absolute stereochemistry of (+)-*proto*-quercitol (102)

1,2:3,4-Di-*O*-isopropylidene-5*R*-(+)-*proto*-quercitol (103)

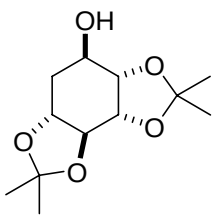

To a solution of (+)-*proto*-quercitol (**102**) (64 mg, 0.39 mmol) in DMF (4 mL) were added 2,2-dimethoxypropane (480 µL, 3.90 mmol) and *p*-toluenesulfonic acid monohydrate (7.4 mg, 0.039 mmol) and the mixture was stirred for 1 h at 80 °C and

warmed to room temperature for 24 h. After the reaction is completed, the reaction mixture was diluted with distilled water and extracted with EtOAc (3 × 50 mL). The combined organic layers were then washed with brine, dried over Na_2SO_4, filtered and concentrated under reduced pressure. The residue was chromatographed on a silica gel column using 50% EtOAc-hexane to yield bis-acetonide **103** (71.2 mg, 75%) as a syrup; ^{1}H NMR ($CDCl_3$, 400 MHz) δ 4.26 (dd, J = 8, 6.4 Hz, 1H), 4.20 (ddd, J = 8, 5.6, 5.2 Hz, 1H), 4.13 (dd, J = 5.6, 5.6 Hz, 1H), 3.70 (ddd, J = 10.4, 10.2, 6.3 Hz, 1H), 3.53 (dd, J = 10, 8.4 Hz, 1H), 1.92-2.06 (m, 2H), 1.44 (s, 3H), 1.36 (s, 3H), 1.35 (s, 3H), 1.29 (s, 3H); ^{13}C NMR ($CDCl_3$, 100 MHz) δ 111.3, 109.8, 81.1, 79.8, 76.1, 72.1, 68.7, 32.3, 27.8, 27.0, 26.9, 25.5.

For the modified Mosher's analysis, (*R*)-α-methoxy-α-(trifluoromethyl)-phenylacetyl chloride (5 µL, 26 µM) was added to 5 mg of bis-acetonide **103** in 10 µL of dry pyridine. After being stirred at room temperature for 3 h, the mixture was extracted with CH_2Cl_2 (3 × 2 mL), washed with 1M HCl (3 × 2 mL), dried over anhydrous Na_2SO_4, filtered and concentrated under reduced pressure. The residue was purified by silica gel column using 30% EtOAc-hexane to give *S*-(-)-MTPA ester (**103a**); ^{1}H NMR ($CDCl_3$, 400 MHz) δ 7.36-7.43 (m, 5H), 5.57 (br s, 1H), 4.07-4.14 (m, 2H), 3.42-3.50 (m, 2H), 3.45 (s, 3H), 1.98-2.18 (m, 2H), 1.45 (s, 3H), 1.36 (s, 3H), 1.32 (s, 3H), 1.27 (s, 3H); ^{13}C NMR ($CDCl_3$, 100 MHz) δ 129.9, 128.6, 127.3, 111.4, 110.2, 81.4, 76.4, 76.2, 72.2, 71.1, 30.4, 28.0, 26.9, 26.8, 25.9.

R-(+)-MTPA ester (**103b**) was also prepared in the same manner using (*S*)-α-methoxy-α-(trifluoromethyl)-phenylacetyl chloride; ^{1}H NMR ($CDCl_3$, 400 MHz) δ 7.46-7.34 (m, 5H), 5.46 (br d , J = 4.8 Hz, 1H), 4.27 (dd, J = 7.2, 6.8 Hz, 1H), 4.12 (dd, J = 6, 6 Hz, 1H), 3.70 (dt, J = 10, 7.2 Hz, 1H), 3.51 (s, 3H), 3.41 (dt, J = 10.2, 6 Hz, 1H), 1.99-2.10 (m, 2H), 1.45 (s, 3H), 1.35 (s, 3H), 1.30 (s, 3H), 1.29 (s, 3H); ^{13}C NMR ($CDCl_3$, 100 MHz) δ 129.8, 128.5, 127.1, 111.7, 110.4, 80.9, 76.5, 76.0, 72.6, 71.6, 29.9, 27.9, 26.9, 26.8, 25.7.

2.5.5 Synthesis of 5-amino-1,2,3,4-cyclohexanetetrols

1,2:3,4-Di-*O*-isopropylidene-5*R*-*O*-mesyl-(+)-*proto*-quercitol (108)

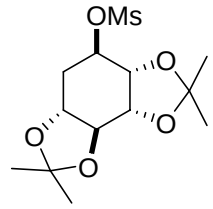

To a 273.2 mg (1.12 mmol) portion of **103** in CH_2Cl_2 (12 mL) was added DMAP (trace amount) and triethylamine (1.3 mL, 8.94 mmol). The mixture was cooled to 0 °C. Mesyl chloride (261 µL, 3.35 mmol) was added slowly and the mixture was stirred for 3 h at room temperature. The product was extracted with CH_2Cl_2 (3 × 50 mL), washed with brine, dried over anhydrous Na_2SO_4, filtered and concentrated under reduced pressure. The crude product was purified by silica gel chromatography (50% EtOAc-hexane) to give **108** (317.2 mg, 88%) as crystalline solid; ^{1}H NMR ($CDCl_3$, 400 MHz) δ 5.03 (dt, J = 6.0, 5.4 Hz, 1H), 4.34 (br d, J = 6.0 Hz, 2H), 3.69 (dt, J = 10.4, 6.4 Hz, 1H), 3.60 (m, 1H), 3.07 (s, 3H), 2.31 (m, 1H), 2.21 (m, 1H), 1.89 (m, 1H), 1.50 (s, 3H), 1.41 (s, 6H), 1.34 (s, 3H).

5*S*-Azido-5-deoxy-1,2:3,4-di-*O*-isopropylidene-(+)-*proto*-quercitol (109)

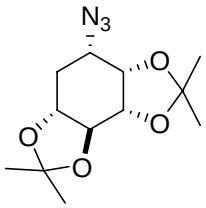

A mixture of **108** (229.7 mg, 0.71 mmol), sodium azide (465.0 mg, 7.12 mmol), 15-crown-5-ether (1.5 mL, 7.12 mmol), and DMF (7 mL) was stirred for 24 h at 100 °C. The reaction mixture was extracted with EtOAc (3 × 100 mL), washed with brine for several times, dried over anhydrous Na_2SO_4, filtered and concentrated under reduced pressure. The residue was chromatographed on a column of silica gel (30% EtOAc-hexane) to give the azide **109** (151.8 mg, 79%) as a crystalline solid; ^{1}H NMR ($CDCl_3$, 400 MHz) δ 4.35 (dd, J = 4.8, 4.8 Hz, 1H), 4.14 (dd, J = 8.4, 5.6 Hz, 1H), 3.58-3.68 (m, 2H), 3.30 (dt, J = 10.6, 4.4 Hz, 1H), 2.30 (m, 1H), 1.89 (m, 1H), 1.52 (s, 3H), 1.37 (s, 3H), 1.35 (s, 3H), 1.33 (s, 3H); ^{13}C NMR ($CDCl_3$, 100 MHz) δ 111.7, 110.6, 81.0, 76.3, 76.2, 73.1, 57.2, 29.1, 27.9, 26.9, 26.8, 25.9.

5*S*-Amino-5-deoxy-1,2:3,4-di-*O*-isopropylidene-(+)-*proto*-quercitol (110)

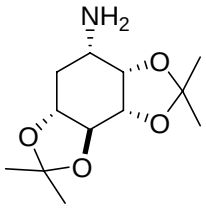

To a cool solution of the azide **109** (33.6 mg, 0.12 mmol) in THF (1.2 mL) at 0 °C was added $LiAlH_4$ (480 µL, 1 M, 0.48 mmol) dropwise. The mixture was stirred for 3 h, diluted with 1 M $NaHCO_3$, extracted by EtOAc (3 × 30 mL), washed with brine,

dried over Na_2SO_4, filtered and concentrated under reduced pressure. The residue was purified by flash chromatography using 20% MeOH-EtOAc to yield an amine **110** (20.7 mg, 71%) as pale yellow oil; ^{1}H NMR (CD_3OD, 400 MHz) δ 4.23 (dd, J = 4.8, 4.4 Hz, 1H), 4.07 (dd, J = 8.4, 4.8 Hz, 1H), 3.41 (dd, J = 9.0, 9.0 Hz, 1H), 3.30 (dt, J = 10.6, 3.2 Hz, 1H), 3.13 (dt, J = 11.6, 4.8 Hz, 1H), 2.08 (m, 1H), 1.51 (dt, J = 11.6, 11.6 Hz, 1H), 1.41 (s, 3H), 1.29 (s, 6H), 1.27 (s, 3H); ^{13}C NMR (CD_3OD, 100 MHz) δ 110.5, 109.0, 82.5, 77.7, 76.4, 74.1, 48.6, 32.8, 27.5, 25.8, 25.1.

5*S*-Amino-1,2,3,4-cyclohexanetetrol (111)

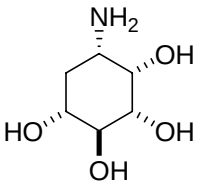

Compound **110** (24.3 mg, 0.10 mmol) was treated with trifluoroacetic acid (77 µL, 1.00 mmol) in THF (1 mL) for 3 h at room temperature. The mixture was evaporated under reduced pressure, washed with EtOAc (3 × 10 mL). The product was dried and evaporated to give compound **111** (17.60 mg, 63%) as colorless oil; ^{1}H NMR (CD_3OD, 400 MHz) δ 3.98 (m, 1H), 3.53 (m, 1H), 3.43 (m, 1H), 3.25-3.29 (m, 2H), 1.94 (m, 1H), 1.87 (m, 1H); ^{13}C NMR (CD_3OD, 100 MHz) δ 74.0, 72.6, 69.4, 69.2, 48.3, 30.7; HRESIMS *m/z* 164.0921 $[M+H]^+$ (calcd for $C_6H_{13}NO_4$+H, 164.0923).

1,2:3,4-Di-*O*-isopropylidene-5-cyclohexanone (112)

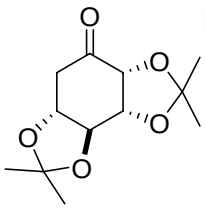

To a solution of **103** (585.2 mg, 2.39 mmol) in DMSO (18 mL, 265.8 mmol) was added acetic anhydride (23 mL, 239.5 mmol) for 5 h at room temperature. The reaction mixture was extracted with EtOAc (3 × 200 mL), washed with brine for several times, dried over anhydrous Na_2SO_4, filtered and concentrated under reduced pressure. The crude product was purified by silica gel column (20% EtOAc-hexane) to give **112** (316.8 mg, 55%) as colorless powder; ^{1}H NMR ($CDCl_3$, 400 MHz) δ 4.59 (dd, J = 8.4, 8.0 Hz, 1H), 4.43 (d, J = 8.4 Hz, 1H), 4.07 (dt, J = 10.6, 6.8 Hz, 1H), 3.50 (dd, J = 10.4, 7.6 Hz, 1H), 2.93 (dd, J = 18.0, 7.2 Hz, 1H), 2.42 (dd, J = 18.2, 11.0 Hz, 1H), 1.44 (s, 3H), 1.42 (s, 3H), 1.40 (s, 3H), 1.32 (s, 3H); ^{13}C NMR ($CDCl_3$, 100 MHz) δ 203.6, 113.6, 112.3, 82.2, 78.7, 75.2, 70.6, 41.1, 27.1, 27.0, 26.7, 24.7.

1,2:3,4-Di-*O*-isopropylidene-5*S*-(+)-*proto*-quercitol (113)

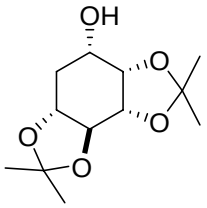

This compound was synthesized from **112** using the same protocol for the synthesis of **110**. The pure compound **113** as crystalline solid (93%); ^{1}H NMR ($CDCl_3$, 400 MHz) δ 4.24-4.32 (m, 2H), 4.10 (m, 1H), 4.00 (dd, *J* = 10.0, 7.6 Hz, 1H), 3.45 (m, 1H), 2.36 (ddd, *J* = 13.2, 6.4, 6 Hz, 1H), 1.89 (ddd, *J* = 13.0, 10.8, 5.2 Hz, 1H), 1.55 (s, 3H), 1.50 (s, 3H), 1.42 (s, 3H), 1.38 (s, 3H).

1,2:3,4-Di-*O*-isopropylidene-5*S*-*O*-mesyl-(+)-*proto*-quercitol (114)

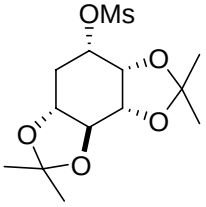

This compound was synthesized from **113** using the same protocol for the synthesis of **108**. The pure compound **114** as crystalline solid (82%); ^{1}H NMR ($CDCl_3$, 400 MHz) δ 4.95 (br d, *J* = 4 Hz, 1H), 4.39 (dd, *J* = 4.8, 4 Hz, 1H), 4.29 (dd, *J* = 7.6, 6.4 Hz, 1H), 3.85 (dd, *J* = 9.6, 8.4 Hz, 1H), 3.07 (s, 3H), 2.51 (dt, *J* = 13.2, 6.4 Hz, 1H), 2.15 (dt, *J* = 12.8, 6.4 Hz, 1H), 1.56 (s, 3H), 1.44 (s, 3H), 1.41 (s, 3H), 1.37 (s, 3H).

5*R*-Azido-5-deoxy-1,2:3,4-di-*O*-isopropylidene-(+)-*proto*-quercitol (115)

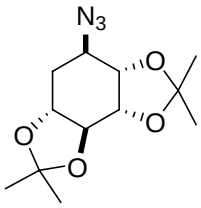

This compound was synthesized from **114** using the same protocol for the synthesis of **109**. The pure compound **115** as crystalline solid (84%); ^{1}H NMR ($CDCl_3$, 400 MHz) δ4.29 (dd, *J* = 6.4, 6.4 Hz, 1H), 4.21 (dd, *J* = 6.4, 6.2 Hz, 1H), 4.02 (dt, *J* = 6.0, 6.0 Hz, 1H), 3.61-3.63 (m, 2H), 2.05-2.08 (m, 2H), 1.51 (s, 3H), 1.42 (s, 3H), 1.41 (s, 3H), 1.35 (s, 3H).

5*R*-Amino-5-deoxy-1,2:3,4-di-*O*-isopropylidene-(+)-*proto*-quercitol (116)

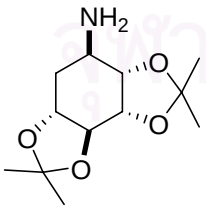

This compound was synthesized from **115** using the same protocol for the synthesis of **110**. The pure compound **116** as colorless oil (43%); ^{1}H NMR (CD_3OD, 400 MHz) δ 4.31 (dd, *J* = 7.0, 7.0 Hz, 1H), 4.10 (dd, *J* = 6.8, 6.8 Hz, 1H), 3.79 (m, 1H), 3.68 (dd, *J* =9.0, 9.0 Hz, 1H), 3.28 (m, 1H), 1.98 (m, 1H), 1.83 (m, 1H), 1.46 (s, 3H), 1.39 (s, 6H), 1.34 (s, 3H).

5*R*-Amino-1,2,3,4-cyclohexanetetrol (117)

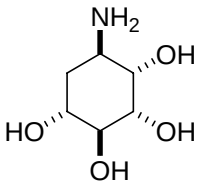

This compound was synthesized from **116** using the same protocol for the synthesis of **111**. The pure compound **117** as colorless oil (86%); ^{1}H NMR (CD_3OD, 400 MHz) δ 3.90-3.95 (m, 2H), 3.78 (m, 1H), 3.53 (m, 1H), 3.38 (m, 1H), 2.06 (m, 1H), 1.95 (m, 1H); ^{13}C NMR (CD_3OD, 100 MHz) δ 73.7, 70.4, 69.8, 69.0, 49.1, 31.1; HRESIMS *m/z* 164.0922 $[M+H]^+$ (calcd for $C_6H_{13}NO_4$+H, 164.0923).

Compounds **118** and **119** were synthesized from **112** and **113**, respectively using the same protocol for the synthesis of **111**.

(1*S*,2*R*,3*S*,4*S*)-Tetrahydroxy-5-cyclohexanone (118)

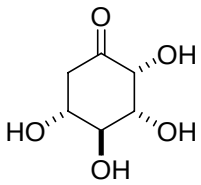

For **118**: as pale pink oil (76%); ^{1}H NMR (DMSO, 400 MHz,) δ 5.46 (br s, 1H), 5.10 (br s, 1H), 4.94 (br s, 2H), 4.27 (br s, 1H), 3.92 (br s, 1H), 3.92 (br s, 1H), 3.81 (br s, 1H), 2.71 (dd, *J* = 12.0, 4.0 Hz, 1H), 2.32 (dd, *J* = 12.0, 4.0 Hz, 1H).

(1*S*,2*R*,3*S*,4*S*,5*S*)-Cyclohexanepentol (119)

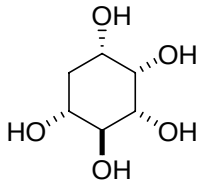

For **119**: as colorless powder (91%); ^{1}H NMR (D_2O, 400 MHz) δ 3.81 (br s, 1H), 3.60 (br d, *J* = 12.4 Hz, 1H), 3.32 (m, 2H), 3.25 (m, 1H), 1.79 (m, 1H), 1.59(m, 1H).

2.5.6 α-Glucosidase inhibition assay

Chemical and equipment

The phosphate buffer (0.1 M), containing 2.84 g of Na_2HPO_4, 2.72 g of KH_2PO_4 were dissolved in 200 mL of distilled water, adjusted to pH 6.9. The α-glucosidase (EC 3.2.1.20) from Baker's yeast was purchased from Sigma-Aldrich (St. Louis, MO, USA). Enzyme was dissolved in phosphate buffer to make 5.7 U/mL stock solution, and further diluted with buffer to get 1 U/mL used for this test. *p*-Nitrophenyl α-D-glucopyranoside was purchased from Sigma-Aldrich as a substrate,

dissolved in phosphate buffer to make 1 mM. Bio-Rad microplate reader model 3550 UV was used to measure the absorbance at 405 nm for the enzymatic reaction in the microplate assay.

Procedure

In the 96-well plate, 10 µL of synthesized compounds (1 mg/mL in DMSO) and 40 µL of 1 U/mL α-glucosidase were added and incubated at 37 °C for 10 min. Then, 50 µL of 1 mM *p*-nitrophenyl α-D-glucopyranoside was added and mixed. The enzyme reaction was carried out at 37 °C for 20 min and then 200 µL of 1 M Na_2CO_3 was added to terminate the reaction. Enzymatic activity was quantified by measuring the absorbance at 405 nm. Percentage inhibition was calculated according to the equation shown below [29].

$$\% \text{ inhibition} = \left(\frac{A_{blank} - A_{sample}}{A_{blank}} \right) \times 100$$

A_{blank} is the absorbance of control without test solution

A_{sample} is the absorbance of sample with test solution

The IC_{50} value was determined from a plot of percentage inhibition versus sample concentration. Acarbose® and DNJ were used as standard controls and the experiment was performed in duplicate.

CHAPTER III

CONCLUSION

In this research, we described efficient synthesis of diastereomerically pure 5*S*- and 5*R*-amino-1,2,3,4-cyclohexanetetrols (**111** and **117**) (Scheme 3.1) which are new analogues of aminocyclitols, starting from naturally available (+)-*proto*-quercitol (**102**) via two parallel routes. The key step involved the exclusive formation of bis-acetonide **103** through selective protection of hydroxyl groups in (+)-*proto*-quercitol. This rationale could be explained by the formation of single *cis*-ketal **120** (Scheme 3.2). In case where several 1,2-acetonides are possible, the formation of *cis*-cyclic ketal is more favorable than *trans*-derivative, thus leading to **103** as a single product. On the other hand, (-)-*vibo*-quercitol (**92**) afforded inseparable mixture of bis-acetonides **93** and **94** [29] on treatment with 2,2-dimethoxypropane though *cis*-cyclic ketal **121**, which was initially generated. This could be rationalized by two possible formations of the second acetonide at C-1/C-2 or C-2/C-3.

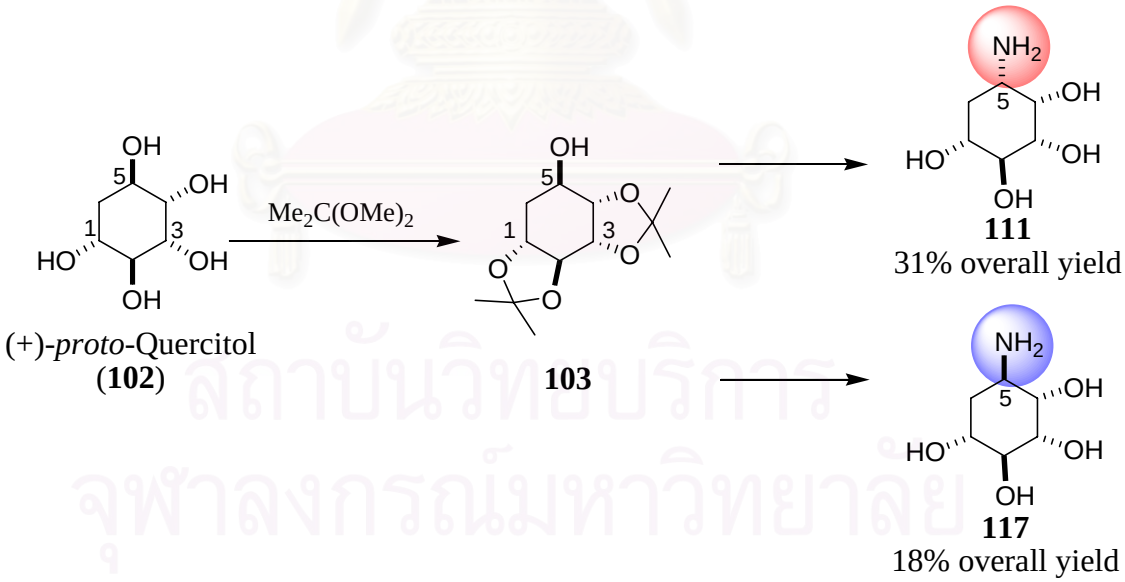

(+)-*proto*-Quercitol
(**102**)

103

Scheme 3.1

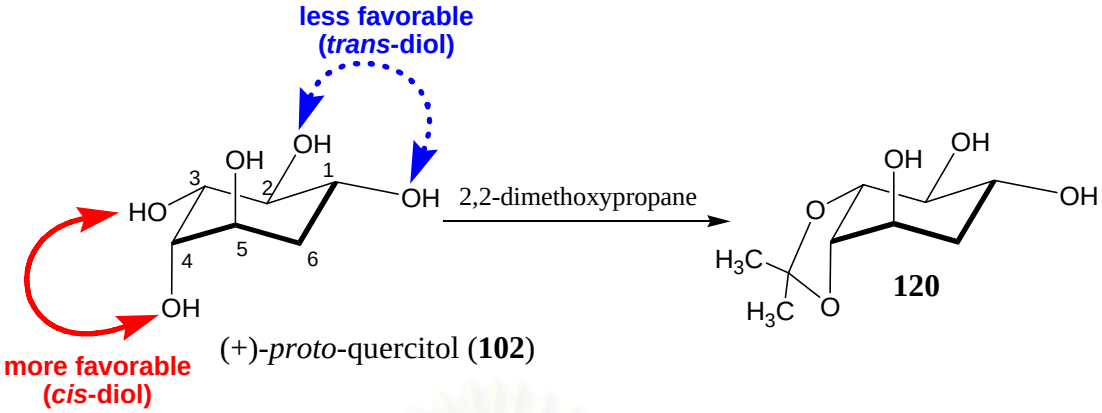

(+)-*proto*-quercitol (**102**)

120

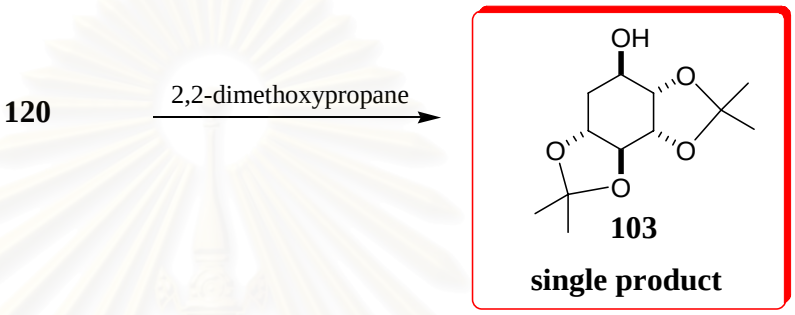

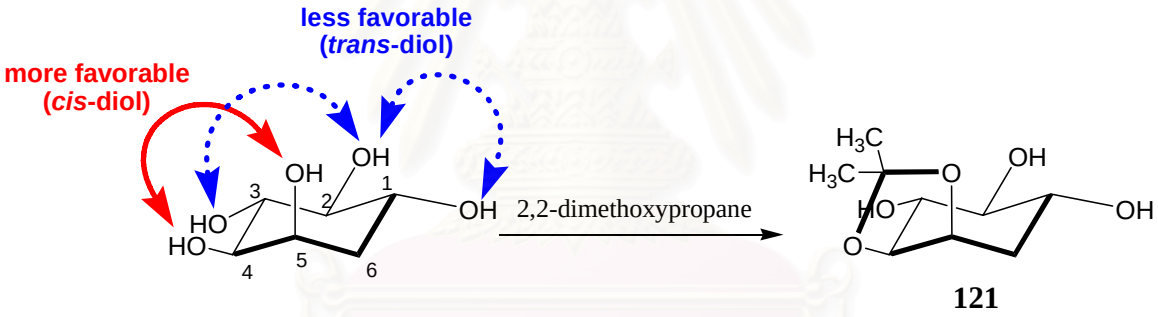

(-)-*vibo*-quercitol **(92)**

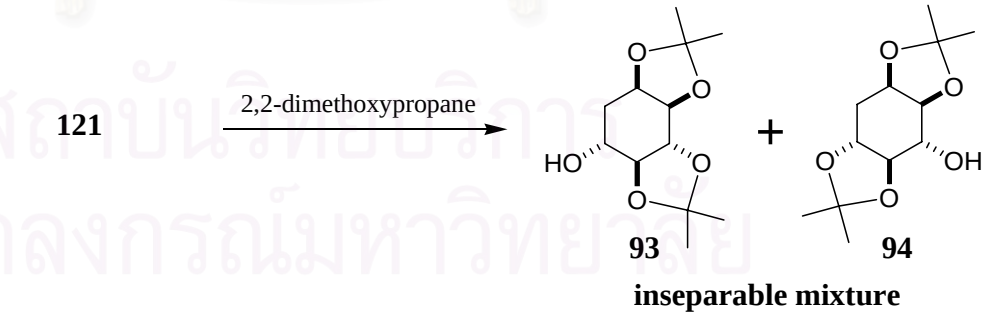

Scheme 3.2

The investigation and evaluation for the α-glucosidase inhibitory activity using colorimetric method indicated that aminocyclitol **117** was the most effective inhibitor with IC_{50} value of 12.5 μM; its inhibition was 45-fold higher than standard drug acarbose. Interestingly, aminocyclitol **117** displayed more striking inhibition than diastereomeric congener **111**, pointing out that configuration at 5-NH_2 is critical for blocking the enzyme. With excellent biological activity of **117**, (+)-*proto*-quercitol would serve as alternative chiral pool for synthesis of diverse aminocyclitols and related analogues. Furthermore, modification of aminocyclitol **117** and study on structure activity relationship will be reported in the future.

REFERENCES

[1] Hermel, A.P.; Mathur, R. *Davidson's Diabetes Mellitus* : *Diagnosis and treatment.* 5th ed. Saunders: Philadelphia, 2004.

[2] Leroith, D.; Taylor, S.I.; Olefsky, J.M. *Diabetes Millitus*: *A fundamental and clinical text.* 3rd ed. Philadeiphia: Lippincott Williams&Wilkins, 2004.

[3] Gravier-Pelletier, C.; Maton, W.; Dintinger, T.; Tellier, C.; Le Merrer, Y. Synthesis and glycosidase inhibitory activity of aminocyclitols with a C6- or a C7-ring. *Tetrahedron* 59(2003) : 8705-8720.

[4] Kumar, P.; Clark, M. *Clinical Medicine*. 6th ed. Elsevier Saunders: Philadeiphia, 2005.

[5] Nolan, J.J. Insulin sensitizers: A new era in the management of type 2 diabetes. In *Diabetes*: *Current perspectives*; Betteridge, D.J., Ed.; Martin Dunitz: London, 2000.

[6] Krentz, A.J.; Bailey, C.J. Oral antidiabetic agents: Current role in type 2 Diabetes mellitus. *Drugs* 65(2005) : 385-411.

[7] Zechel, D.L.; Withers, S.G. Glycosidase mechanisms: Anatomy of a finely tuned catalyst. *Acc. Chem. Res.* 33(2000) : 11-18.

[8] Rhabasa-Lhoret, R.; Chiasson, J. Alpha-glucosidase inhibitors. In *Internaional Textbook of diabetes mellitus*; Defronzo, R.A.; Ferrannini, E.; Keen, H.; Zimmet, P., Ed.; John Wiley: UK, 2004.

[9] Blidi, L.E.; Ahbala, M.; Boltea, J.; Lemaire, M. Straightforward chemo-enzymatic synthesis of new aminocyclitols, analogues of valiolamine and their evaluation as glycosidase inhibitors. *Tetrahedron*: *Asymmetry* 17(2006) : 2684-2688.

[10] Bridges, C.G.; Brennan, T.M.; Taylor, D.L.; McPherson, M.; Tyms, A.S. The prevention of cell adhesion and the cell-to-cell spread castanospermine (MDL 28574). *Antivir*. *Res.* 25(1994) : 169-175.

[11] Fischer, P.B.; Karlsson, G.B.; Dwek, R.A.; Platt, F.M. *N*-butyldeoxynojirimycin-mediated inhibition of human immunodeficiency virus entry correlates with impairment of gp120 shedding and gp41 exposure. *J. Virol*. 70(1996) : 7153-7160.

[12] Borges de Melo, E.; da Silveira Gomes, A.; Carvalho, I. α- and β-Glucosidase inhibitors: Chemical structure and biological activity. *Tetrahedron* 62(2006) : 10277-10302.

[13] Chen, X.; Zheng, Y.; Shen, Y. A new method for production of valienamine with microbial degradation of acarbose. *Biotechnol. Prog.* 21(2005) : 1002-1003.

[14] Bischoff, H. Pharmacology of alpha-glucosidase inhibition. *Eur. J. Clin. Invest.* 24(1994) : 3-10.

[15] Delgado, A. Recent advances in the chemistry of aminocyclitols. *Eur. J. Org. Chem.* (2008) : 3893-3906.

[16] Gomez, A.M.; Moreno, E.; Uriel, C.; Jarosz, S.; Valverde, S.; Lopez, J.C. Novel strategies for the preparation of aminocarbasugar analogues: Syntheses of *N*-substituted aminocyclitols from D-mannose. *Tetrahedron*: *Asymmetry* 16 (2005) : 2401-2407.

[17] Behr, J.B.; Chevrier, C.; Defoin, A.; Tarnus, C.; Streith, J. Asymmetric synthesis of potent glycosidase and very potent α-mannosidase inhibitors: 4-amino-4-deoxy-L-erythrose and 4-amino-4,5-dideoxy-L-ribose. *Tetrahedron* 59(2003) : 543–553.

[18] Lee, Y.J.; Lee, K.; Jung, S.; Jeon, H.B.; Kim, K.S. Synthesis of enantiopure cyclitols from (±)-3-bromocyclohexene mediated by intramolecular oxyselenenylation employing (*S*,*S*)-hydrobenzoin and (*S*)-mandelic acid as chiral sources. *Tetrahedron* 61(2005) : 1987-2001.

[19] Chung, S.-K.; Kwon, Y.-U. Practical synthesis of all inositol stereoisomers from *myo*-inositol. *Bioorg. Med. Chem. Lett*. 9(1999) : 2135-2140.

[20] Arjona, O.; Gmez, A.M.; Lpez, J.C.; Plumet, J. Synthesis and conformational and biological aspects of carbasugars. *Chem. Rev.* 107(2007) : 1919-2036.

[21] Sureshan, K.M.; Ikeda, K.; Asano, N.; Watanabe, Y. Efficient syntheses of optically pure *chiro*- and *allo*-inositol derivatives, azidocyclitols and aminocyclitols from *myo*-inositol. *Tetrahedron* 64(2008) : 4072–4080.

[22] Egido-Gabas, M.; Serrano, P.; Casas, J.; Llebaria, A.; Delgado, A. New aminocyclitols as modulators of glucosylceramide metabolism. *Org. Biomol. Chem.* 3(2005) : 1195–1201.

[23] Shing, T.K.M.; Wan, L.H. Facile syntheses of valiolamine and its diastereomers from (-)-quinic acid. Nucleophilic substitution reactions of 5-(hydroxymethyl)cyclohexane-1,2,3,4,5-pentol. *J. Org. Chem.* 61(1996) : 8468–8479.

[24] Shing, T.K.M.; Tai, V.W.F. Facile syntheses of cyclophellitol and its (1*R*,6*S*)-, (1*R*,2*S*,6*S*)-, (2*S*)-diastereoisomers from (–)-quinic acid. *J. Chem. Soc., Chem. Commun.* (1993) : 995-997.

[25] Kok, S.H.L.; Lee, C.C.; Shing, T.K.M. A new synthesis of valienamine. *J. Org. Chem.* 66 (2001) : 7184–7190.

[26] Shing, T.K.M.; Li, T.Y.; Kok, S.H.L. Enantiospecific syntheses of valienamine and 2-*epi*-valienamine. *J. Org. Chem.* 64(1999) : 1941–1946.

[27] Shih, T.-L.; Lin, Y.-L.; Kuo, W.-S. Highly stereoselective and stereospecific syntheses of a variety of quercitols from D-(-)-quinic acid. *Tetrahedron* 61 (2005) : 1919–1924.

[28] Ogawa, S.; Aoyama, H.; Tezuka, Y. Synthesis of 1-and 3-*C*-(aminomethyl)-1,2,3,4,5-cyclohexanepentols from (+)-*epi*-quercitol. *J. Carbohydr. Chem.* 20 (2001) : 703-717.

[29] Ogawa, S.; Asada, M.; Ooki, Y.; Mori, M.; Itoh, M.; Korenaga, T. Design and synthesis of glycosidase inhibitor 5-amino-1,2,3,4-cyclohexanetetrol derivatives from (-)-*vibo*-quercitol. *Bioorg. Med. Chem.* 13(2005) : 4306-4314.

[30] Phuwapraisirisan, P. Chemical constituents from the stems of *Arfuillea arborescens* Pierre and their biological activity. MS thesis, Chulalongkorn University, 1998.

[31] Kelly, D.R. A new method for the determination of the absolute stereochemistry of aromatic and heteroaromatic alkanols using Mosher's esters. *Tetrahedron*: *Asymmetry* 10(1999) : 2927-2934.

[32] Seco, J.M.; Quio, E.; Riguera, R. The assignment of absolute configuration by NMR. *Chem. Rev.* 104(2004) : 17-117.

[33] Albright, J.D.; Goldman, L. Dimethyl sulfoxide-acid anhydride mixtures for the oxidation of alcohols. *J. Am. Chem. Soc.* 89(1967) : 2416-2423.

[34] Pullela, S.V.; Tiwari, A.K.; Vanka, U.S.; Vummenthula, A.; Tatipaka, H.B.; Dasari, K.R.; Khan, I.A.; Janaswamy, M.R. HPLC assisted chemobiological standardization of α-glucosidase-I enzyme inhibitory constituents from *Piper*

longum Linn-An Indian medicinal plant. *J. Ethnopharmacol*. 108(2006) : 445–449.

APPENDICES

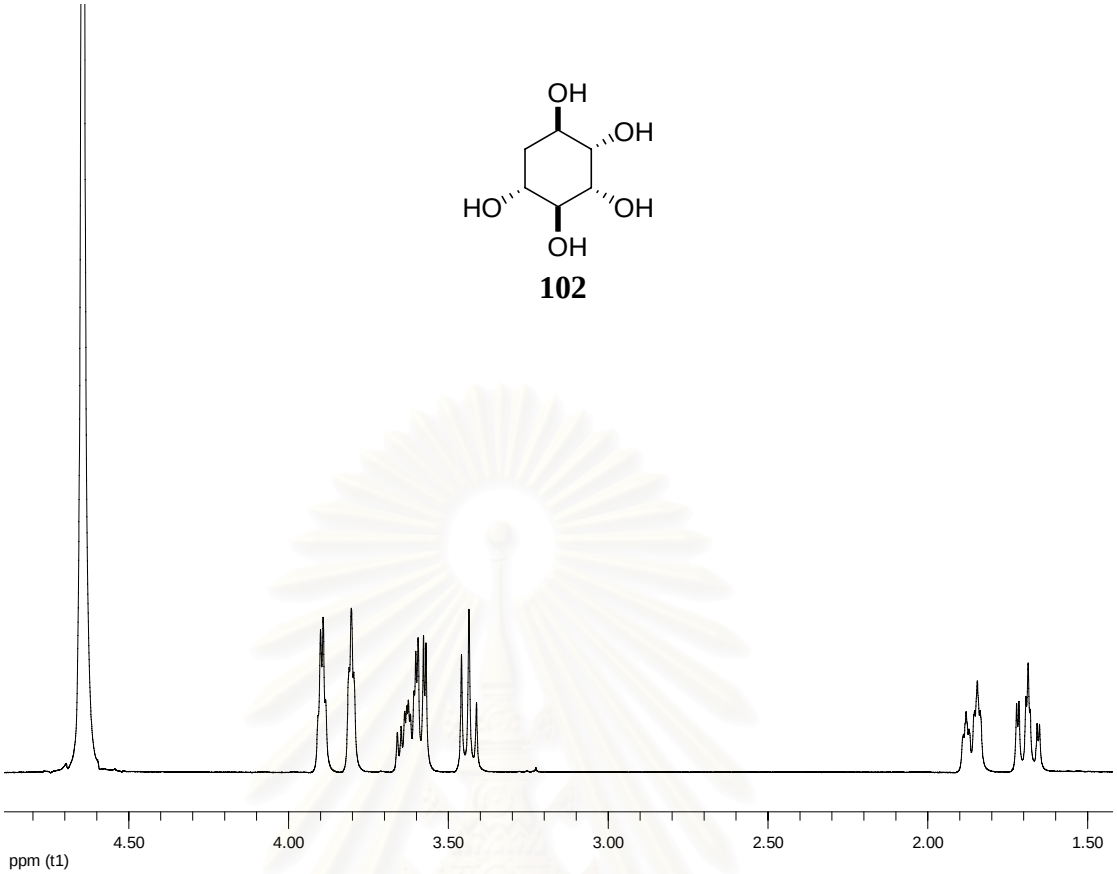

102

Figure 1. The ^{1}H NMR (D_2O) spectrum of **102**.

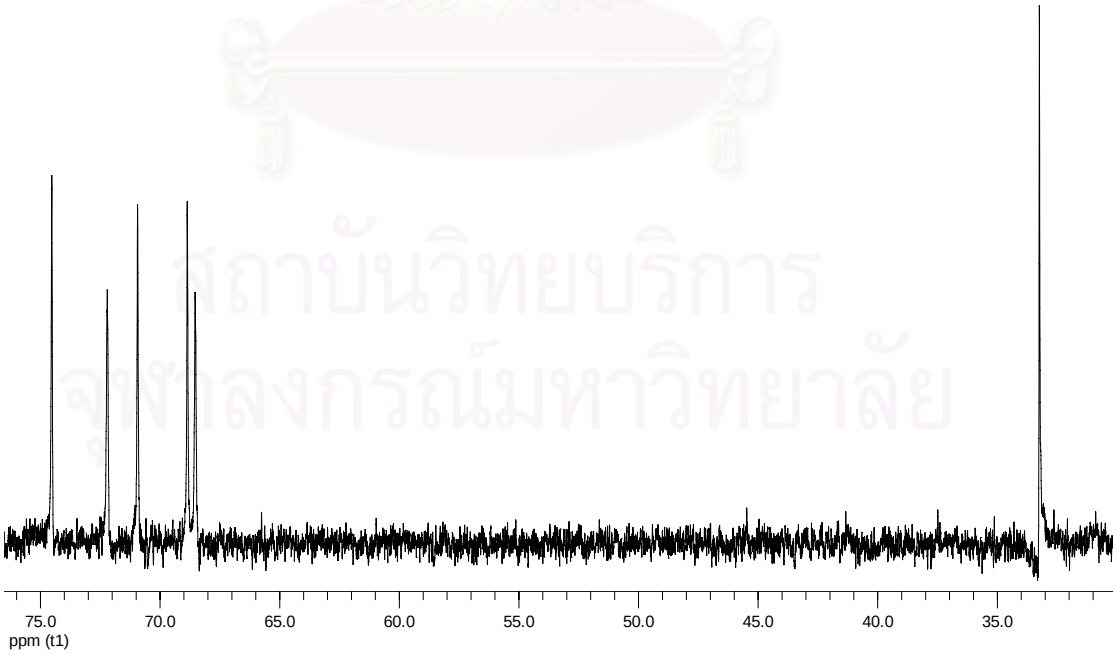

Figure 2. The ^{13}C NMR (D_2O) spectrum of **102**.

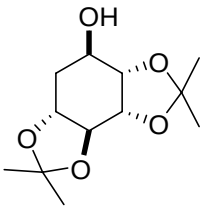

103

Figure 3. The ^{1}H NMR ($CDCl_3$) spectrum of **103**.

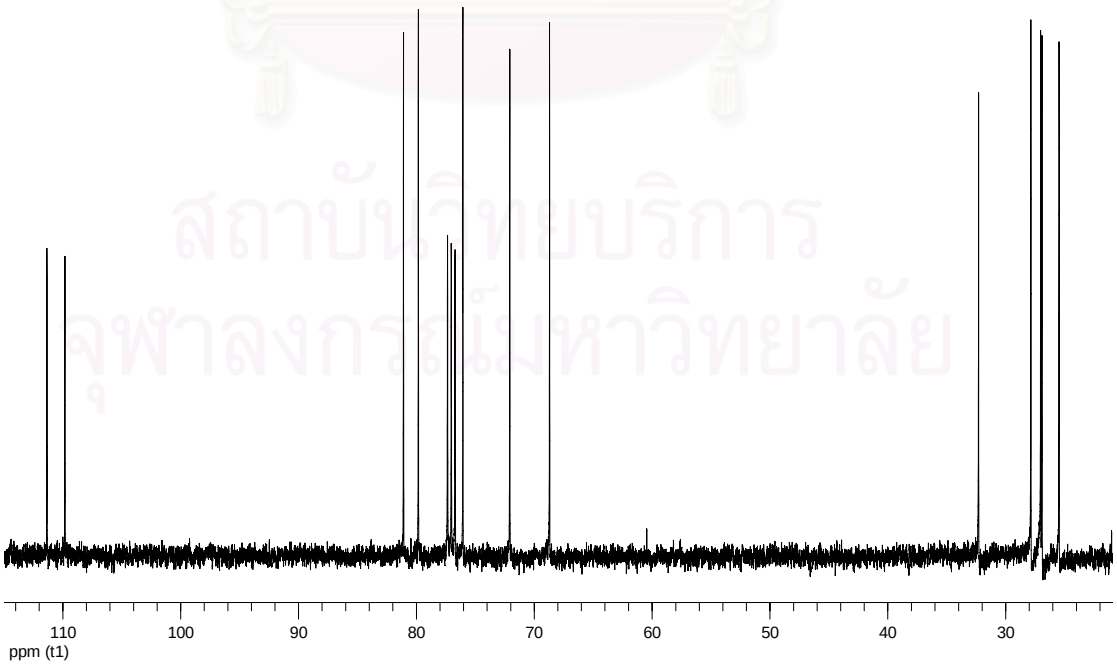

Figure 4. The ^{13}C NMR ($CDCl_3$) spectrum of **103**.

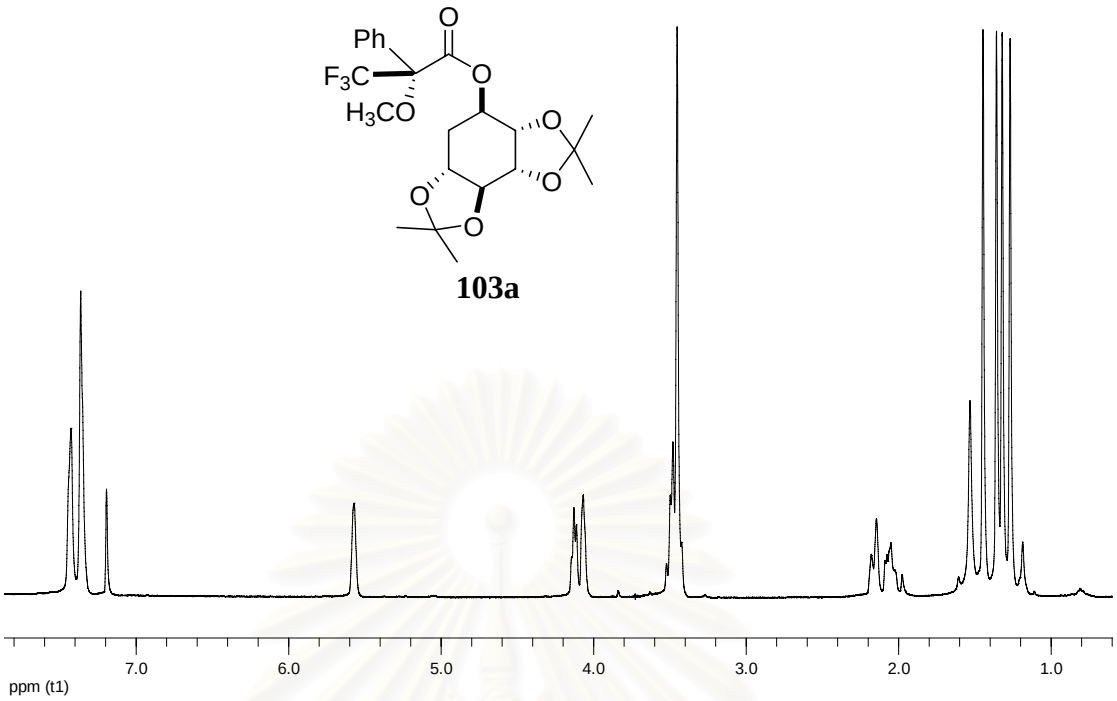

103a

Figure 5. The ^{1}H NMR ($CDCl_3$) spectrum of **103a**.

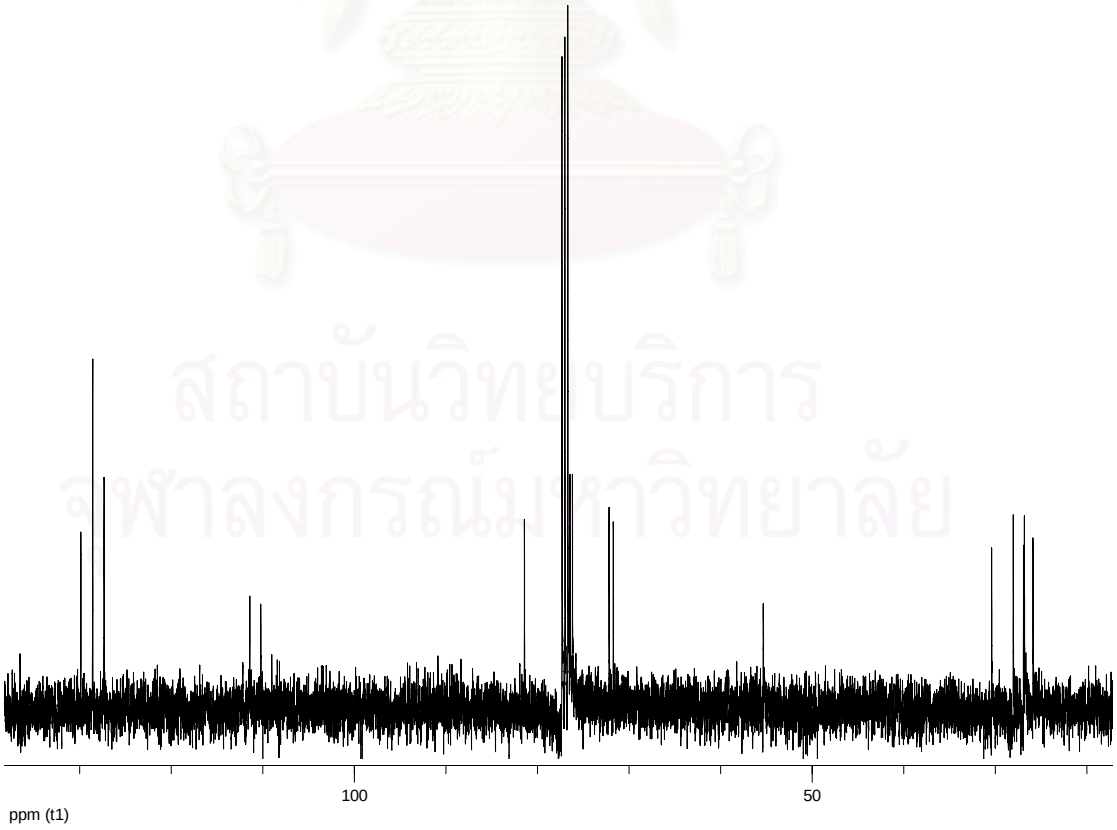

Figure 6. The ^{13}C NMR ($CDCl_3$) spectrum of **103a**.

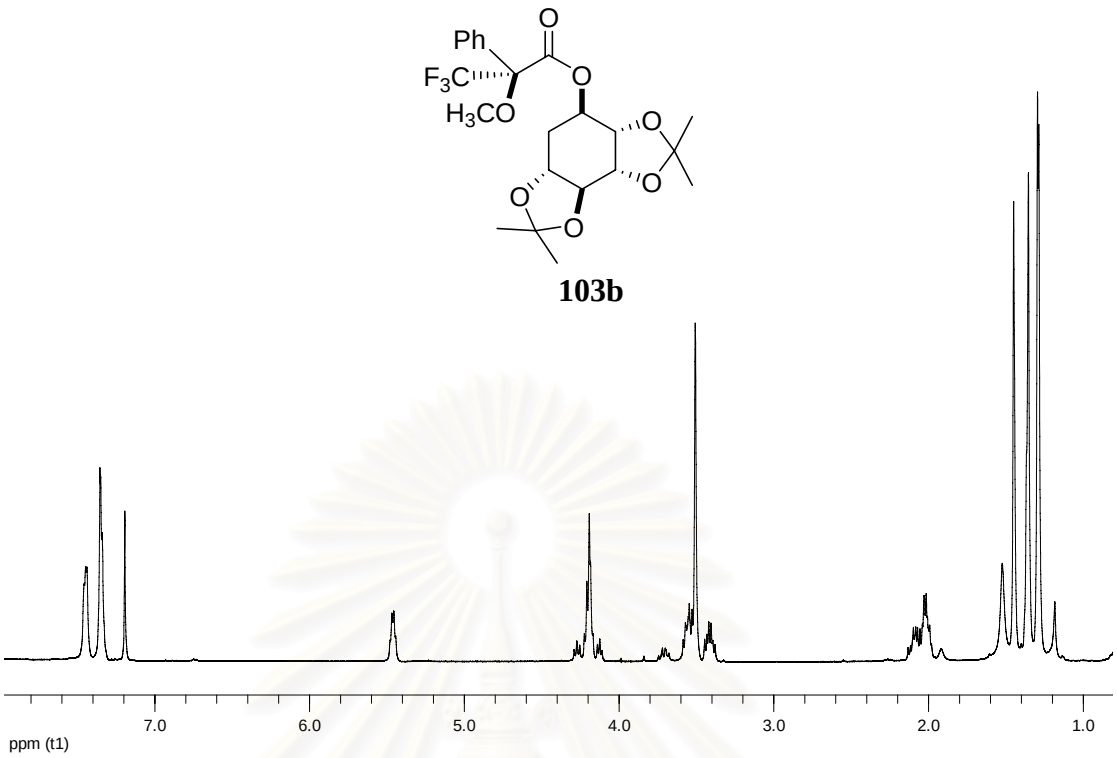

103b

Figure 7. The ^{1}H NMR ($CDCl_3$) spectrum of **103b**.

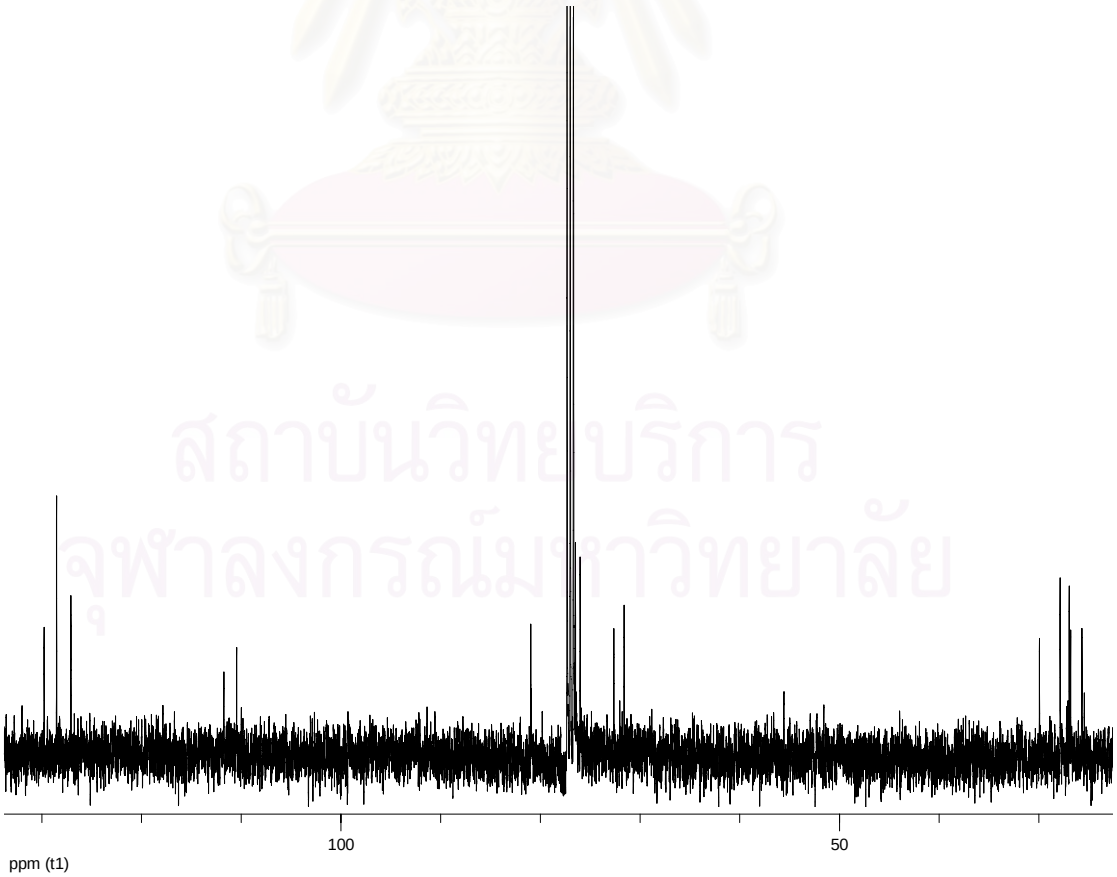

Figure 8. The ^{13}C NMR ($CDCl_3$) spectrum of **103b**.

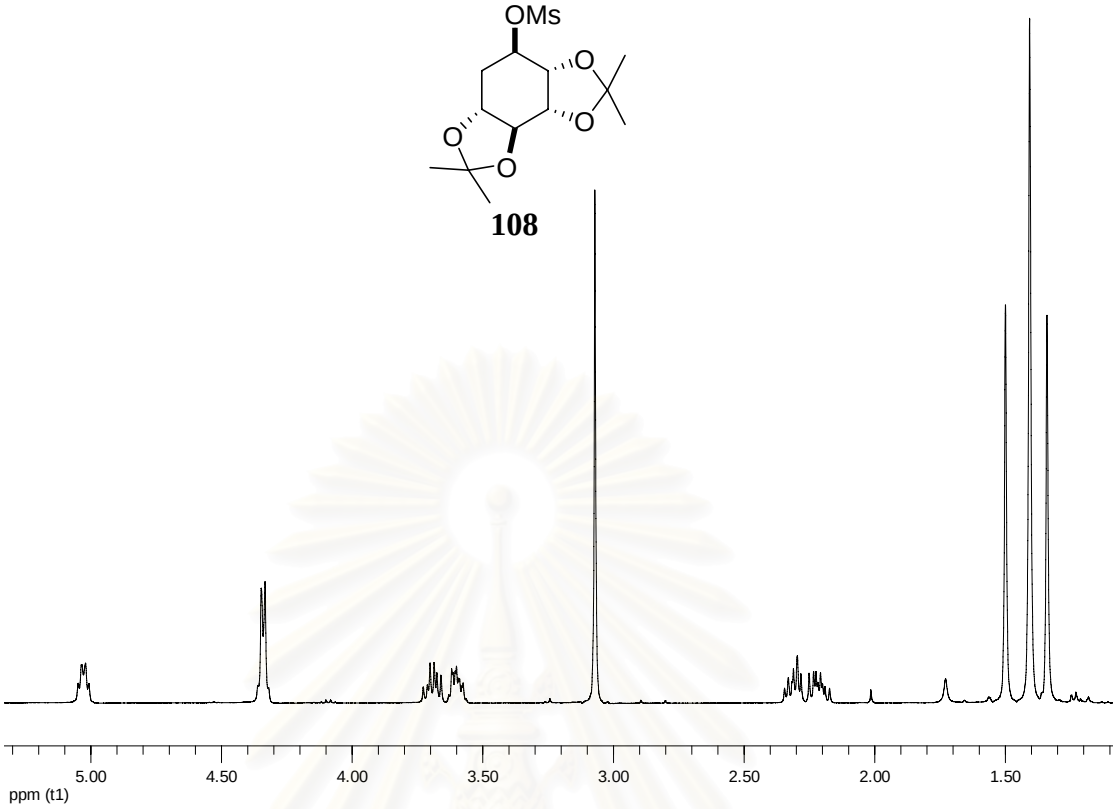

Figure 9. The ^{1}H NMR ($CDCl_3$) spectrum of **108**.

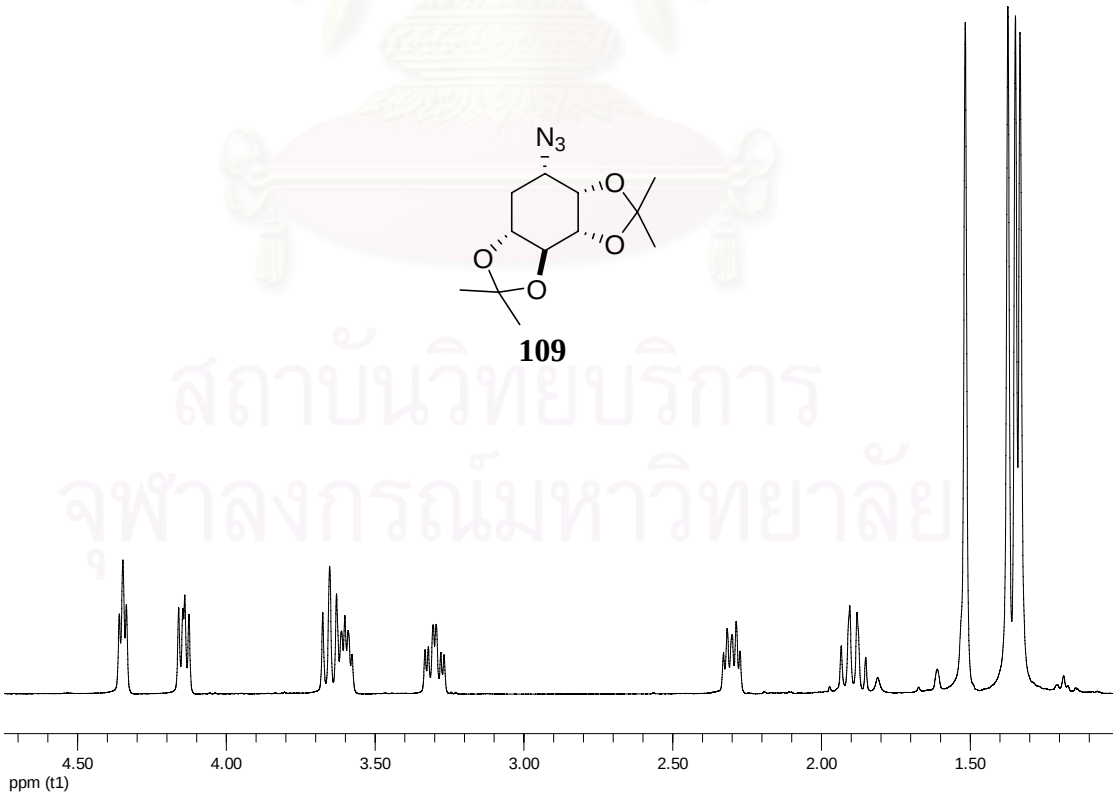

Figure 10. The ^{1}H NMR ($CDCl_3$) spectrum of **109**.

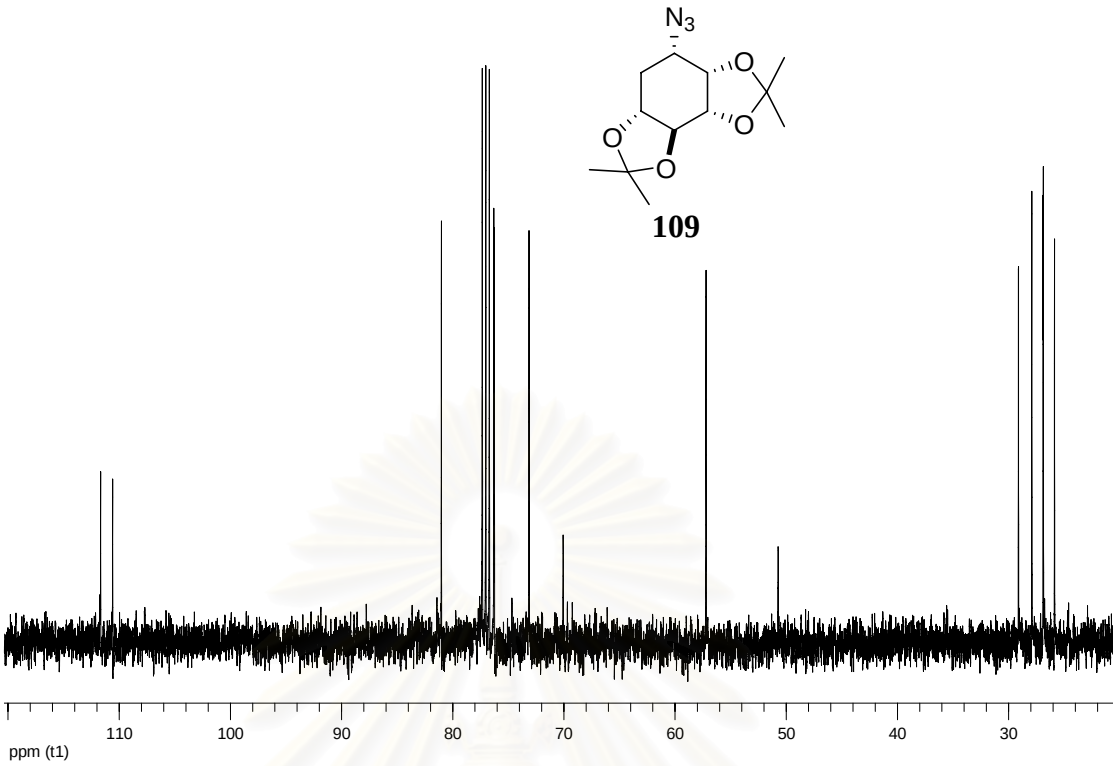

Figure 11. The ^{13}C NMR ($CDCl_3$) spectrum of **109**.

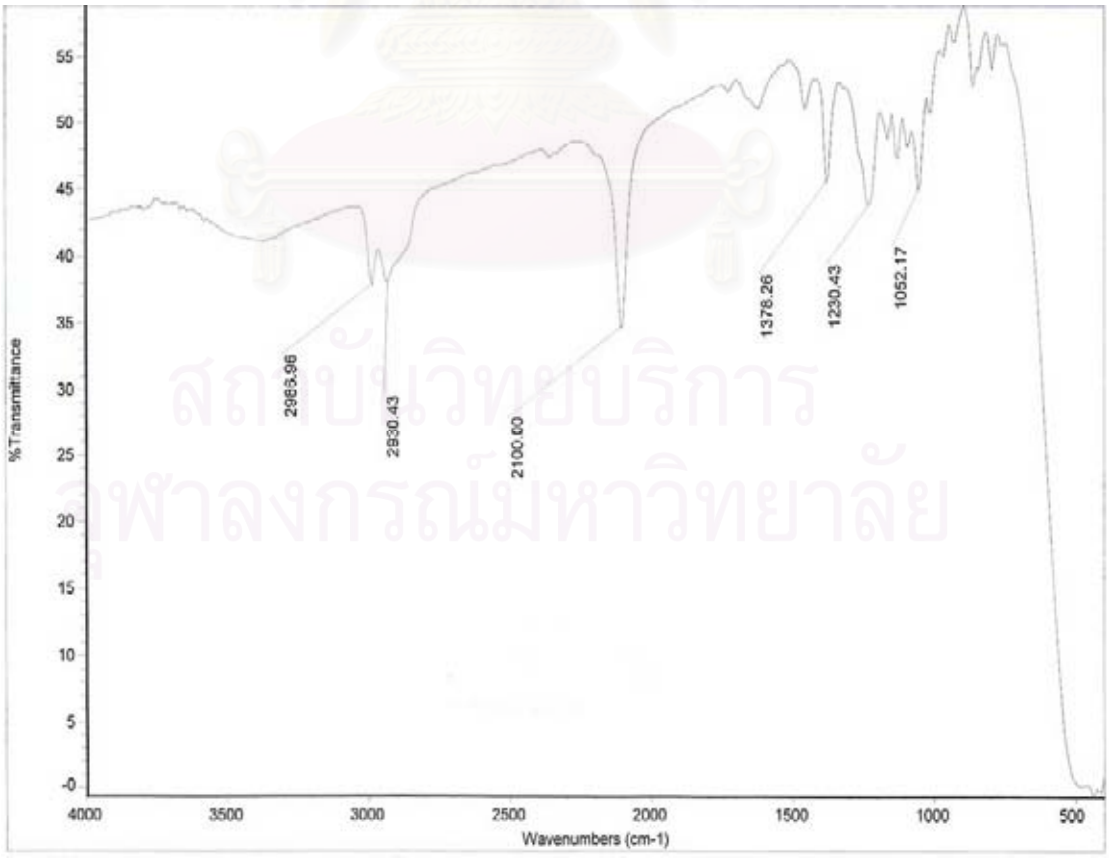

Figure 12. IR spectrum of **109**.

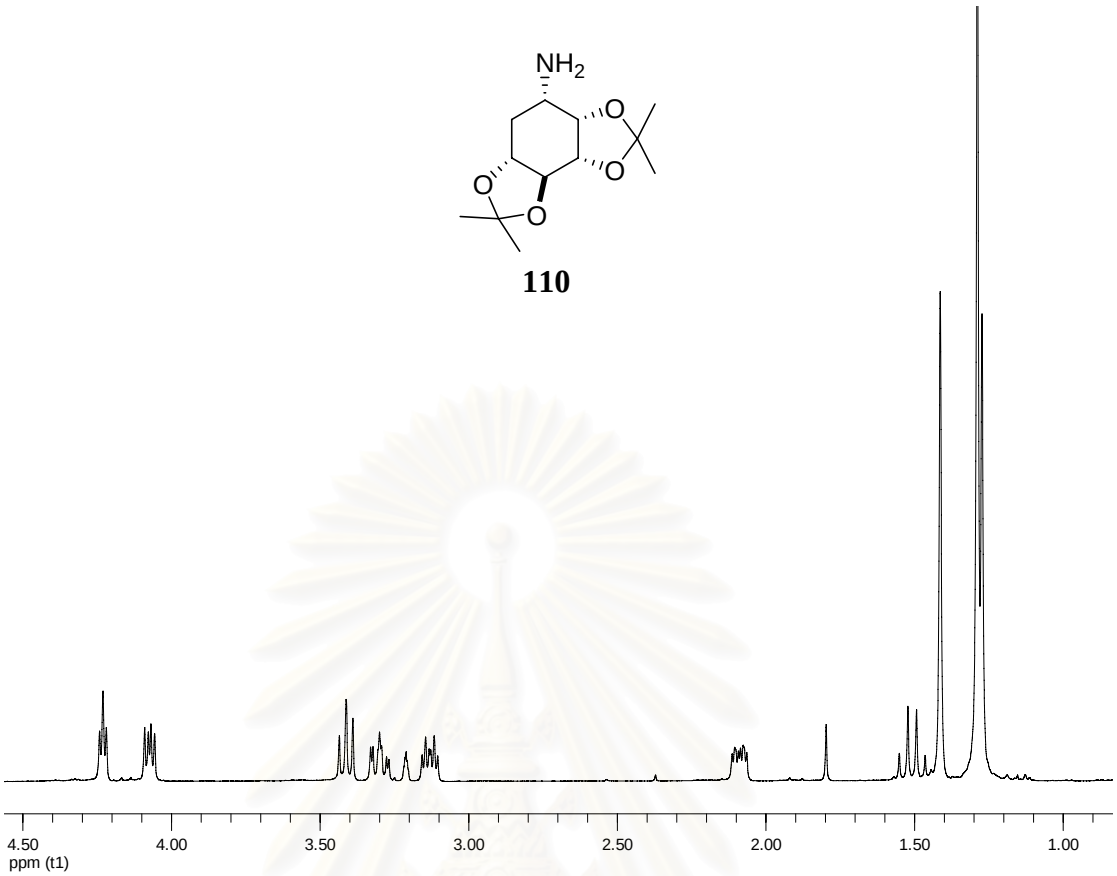

110

Figure 13. The ^{1}H NMR (CD_3OD) spectrum of **110**.

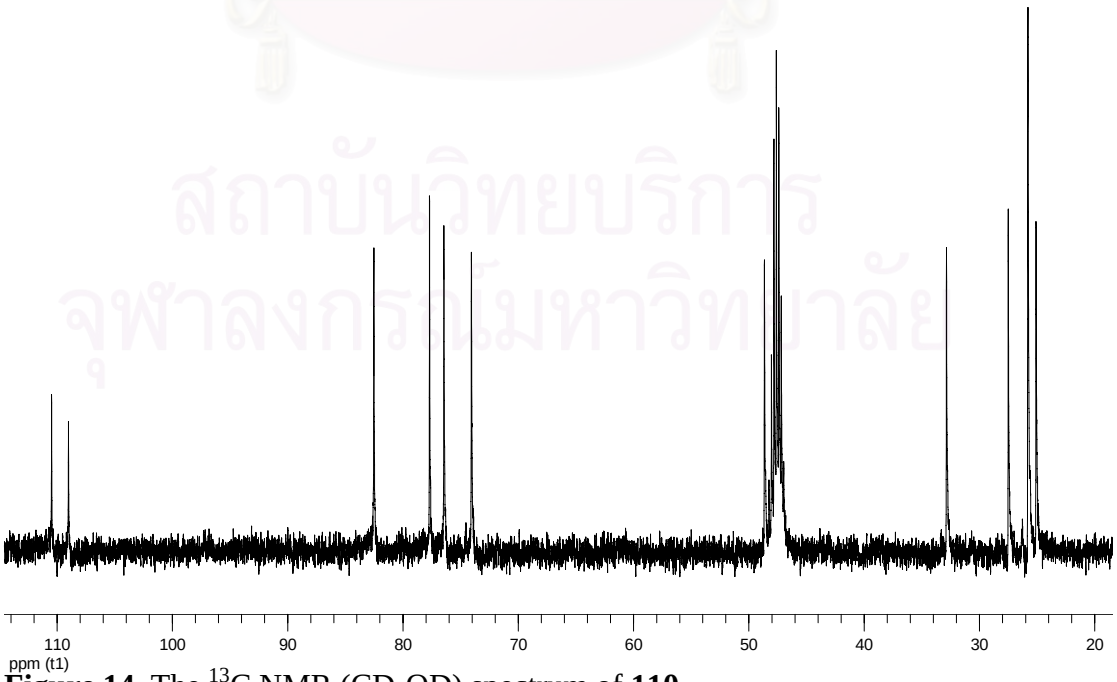

Figure 14. The ^{13}C NMR (CD_3OD) spectrum of **110**.

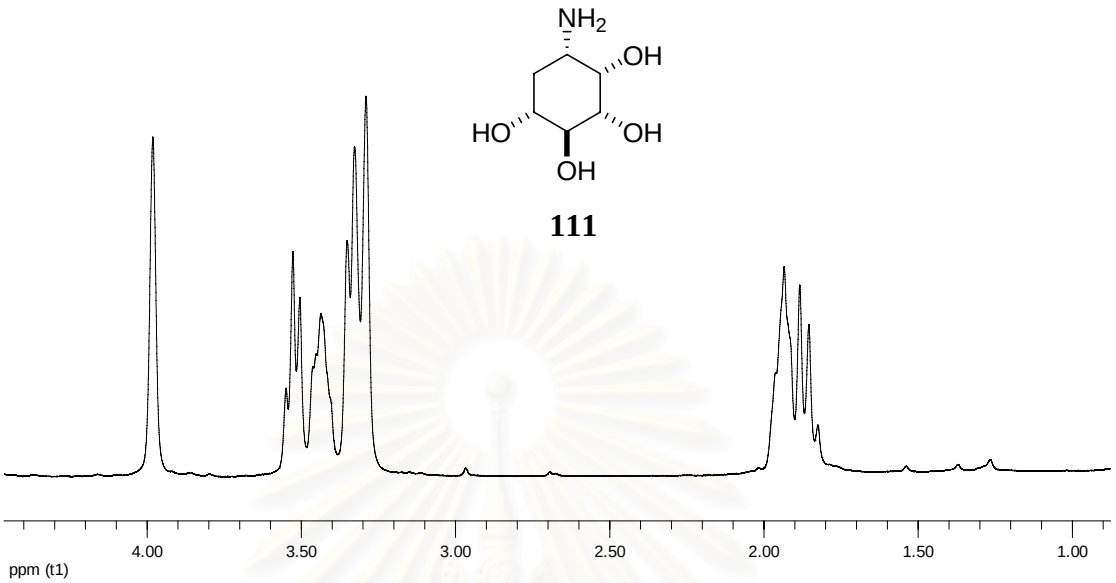

111

Figure 15. The ^{1}H NMR (CD_3OD) spectrum of **111**.

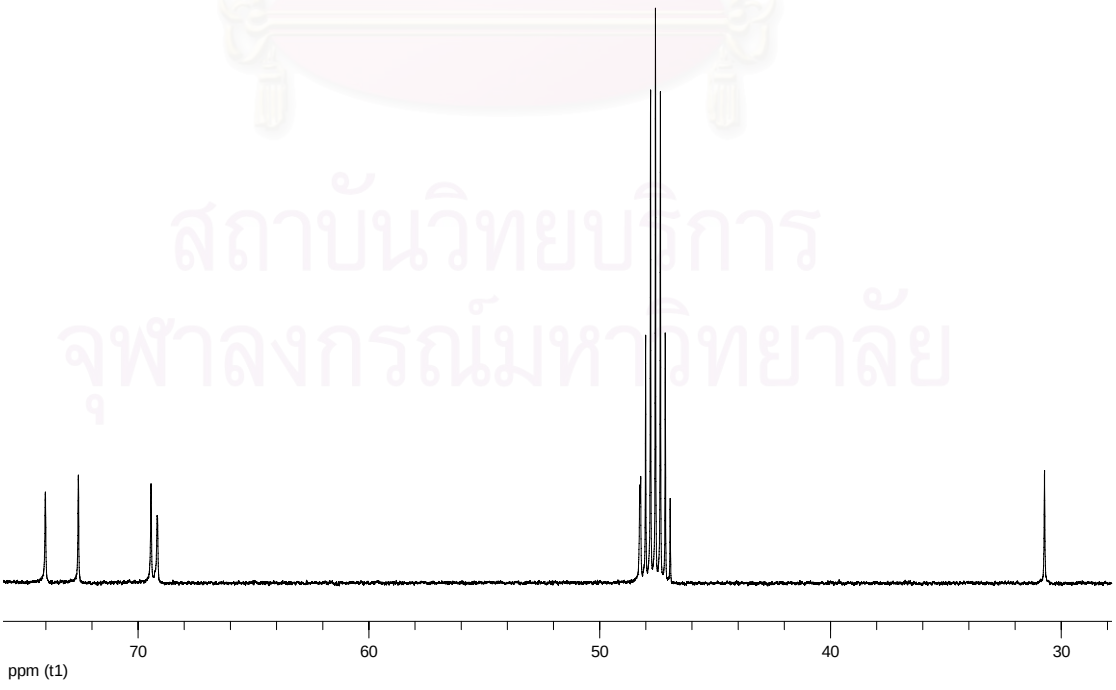

Figure 16. The ^{13}C NMR (CD_3OD) spectrum of **111**.

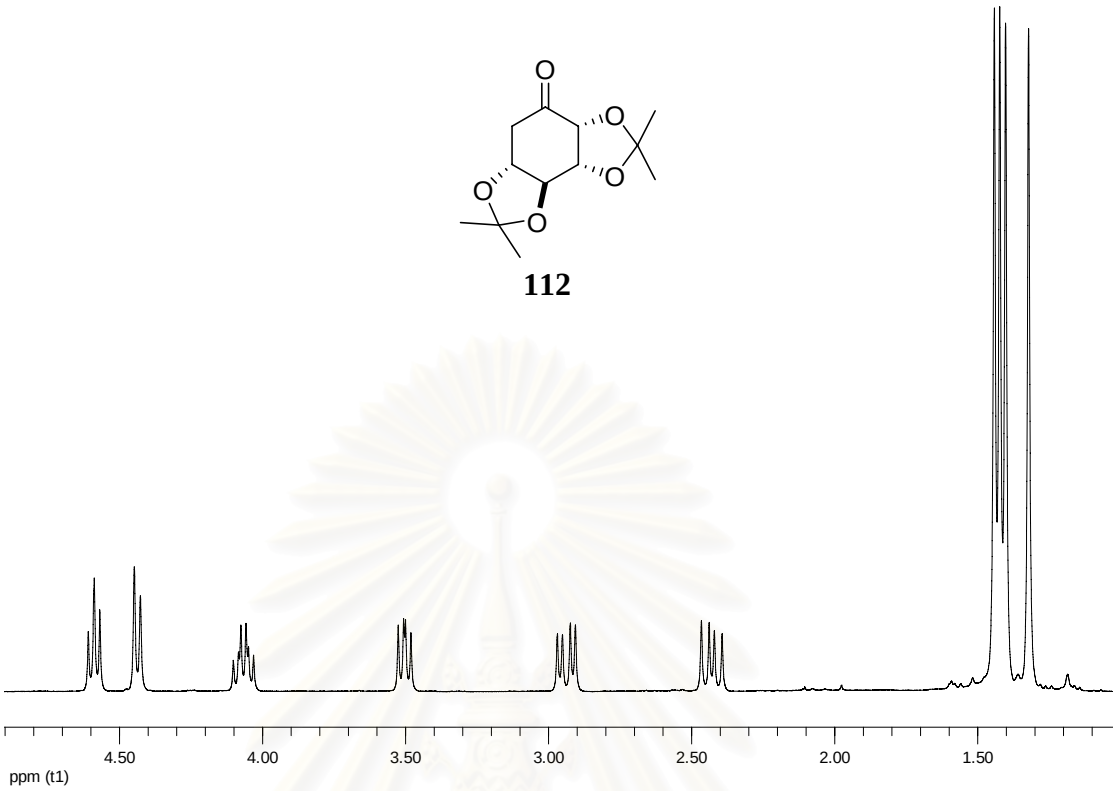

112

Figure 17. The ^{1}H NMR ($CDCl_3$) spectrum of **112**.

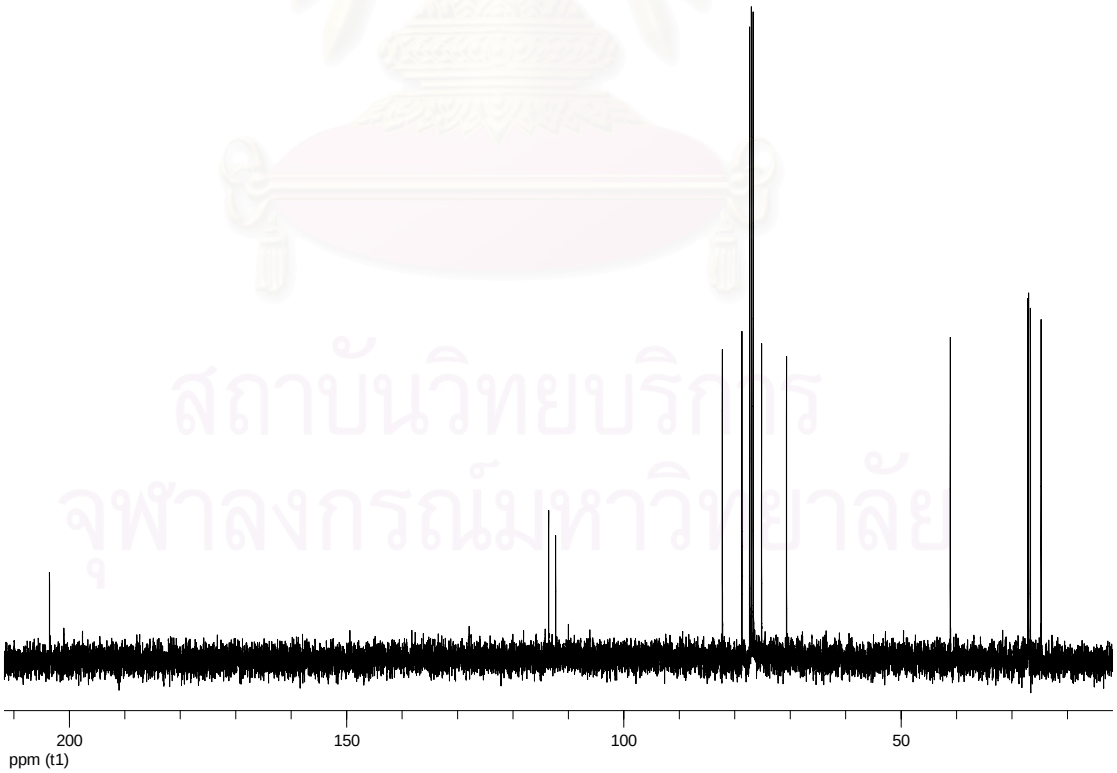

Figure 18. The ^{13}C NMR ($CDCl_3$) spectrum of **112**.

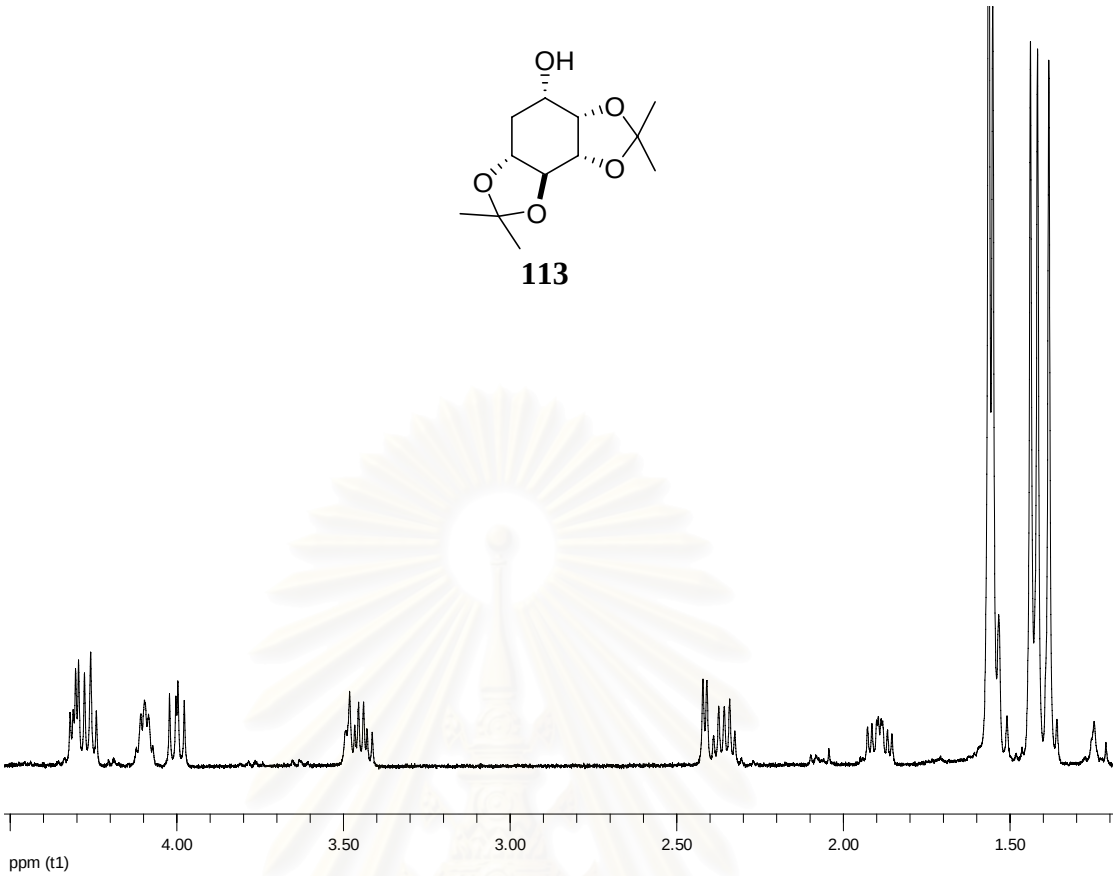

113

Figure 19. The ^{1}H NMR ($CDCl_3$) spectrum of **113**.

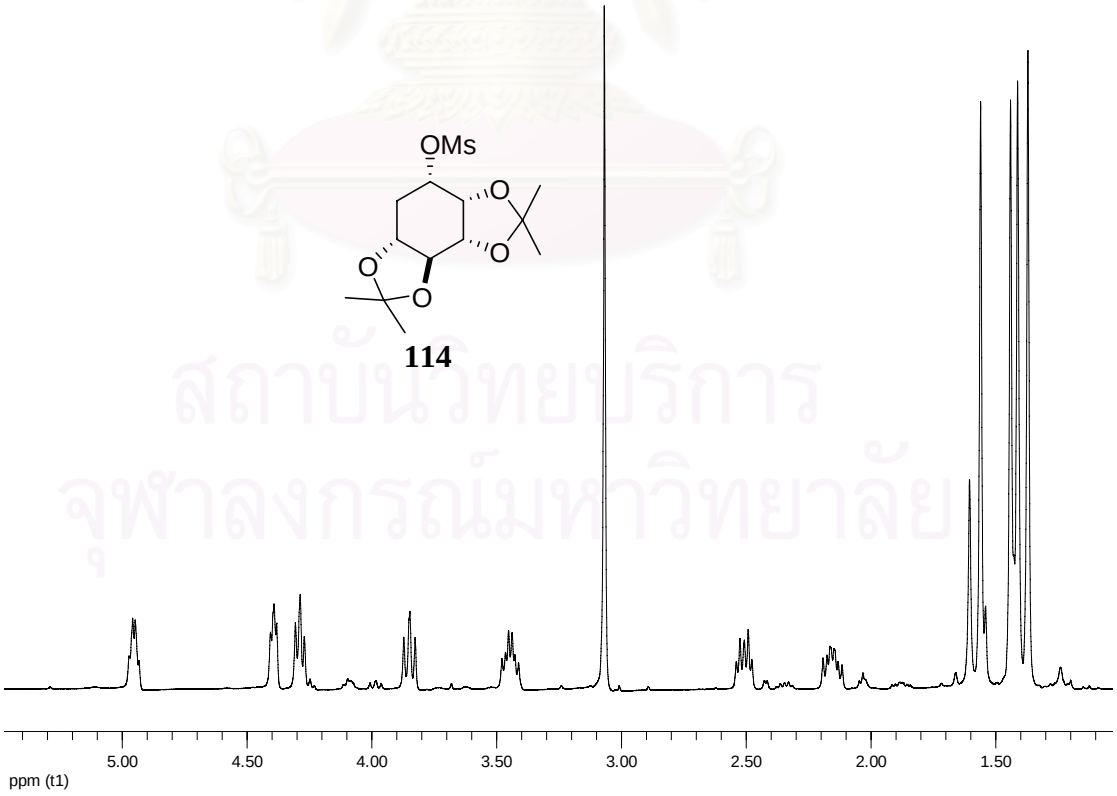

114

Figure 20. The ^{1}H NMR ($CDCl_3$) spectrum of **114**.

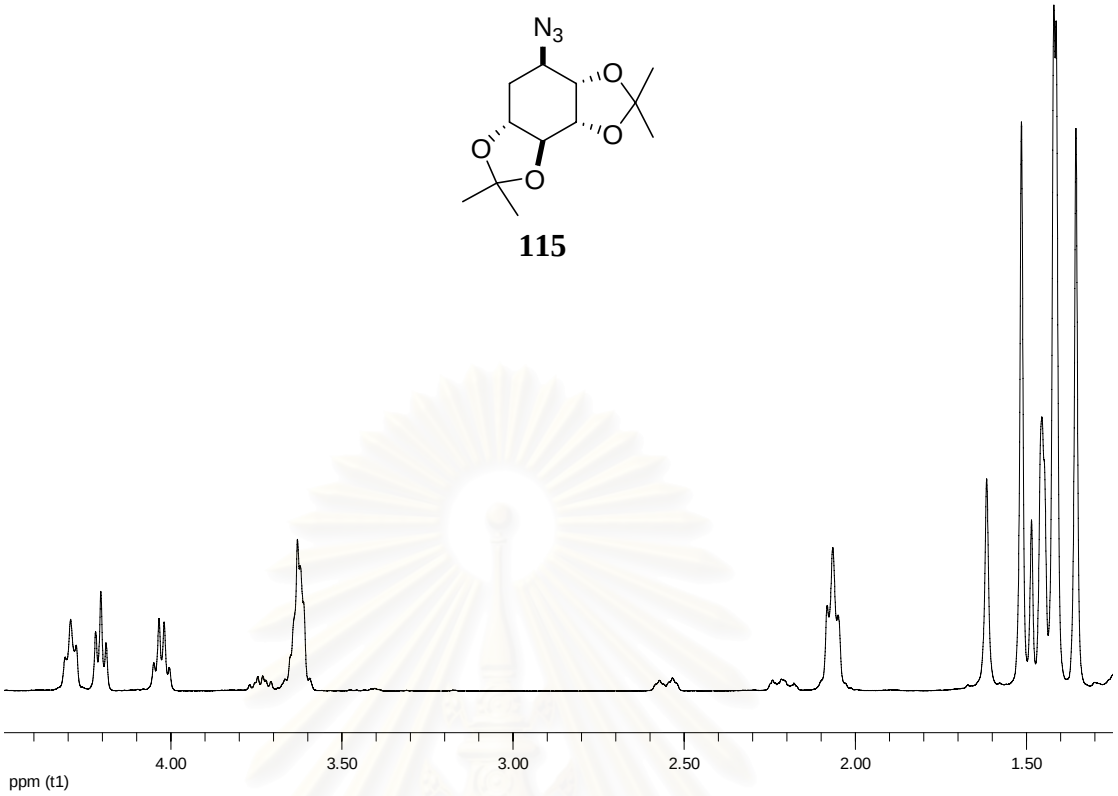

115

Figure 21. The ^{1}H NMR ($CDCl_3$) spectrum of **115**.

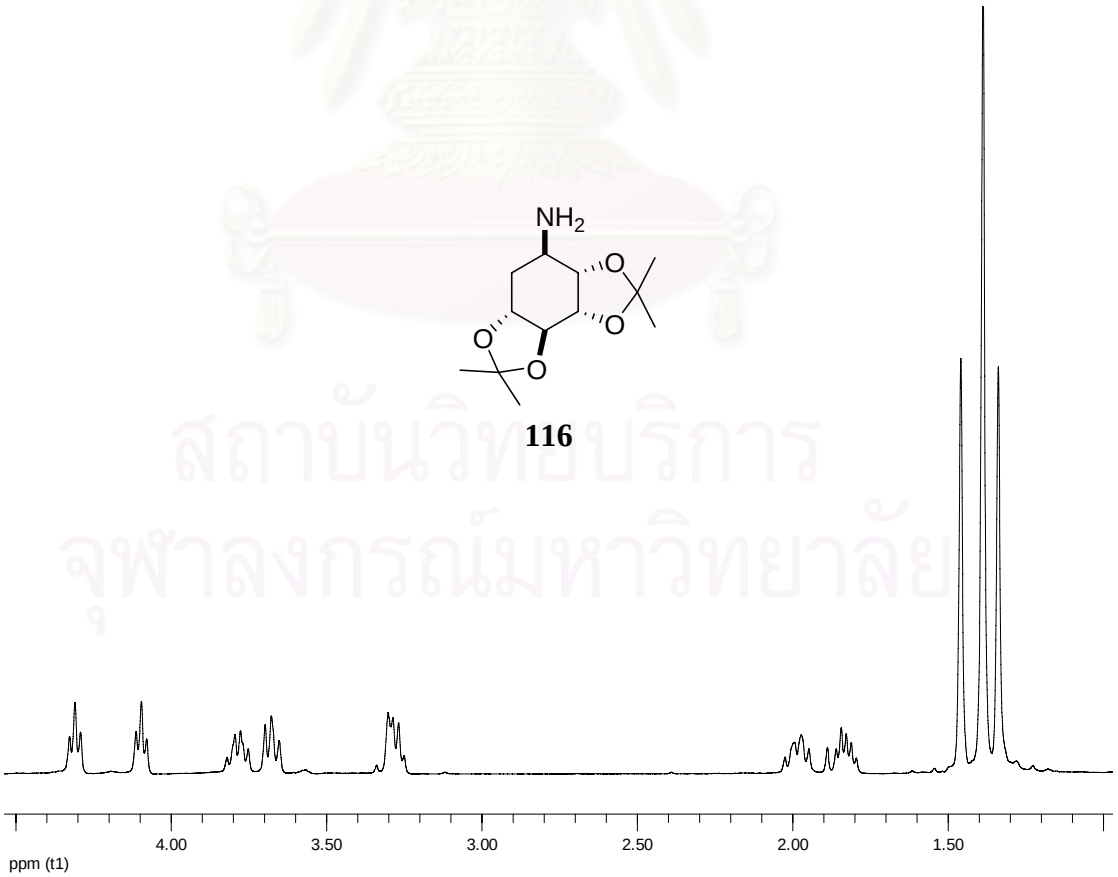

116

Figure 22. The ^{1}H NMR (CD_3OD) spectrum of **116**.

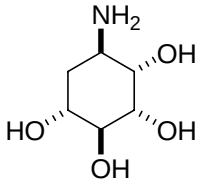

117

Figure 23. The ^{1}H NMR (CD_3OD) spectrum of **117**.

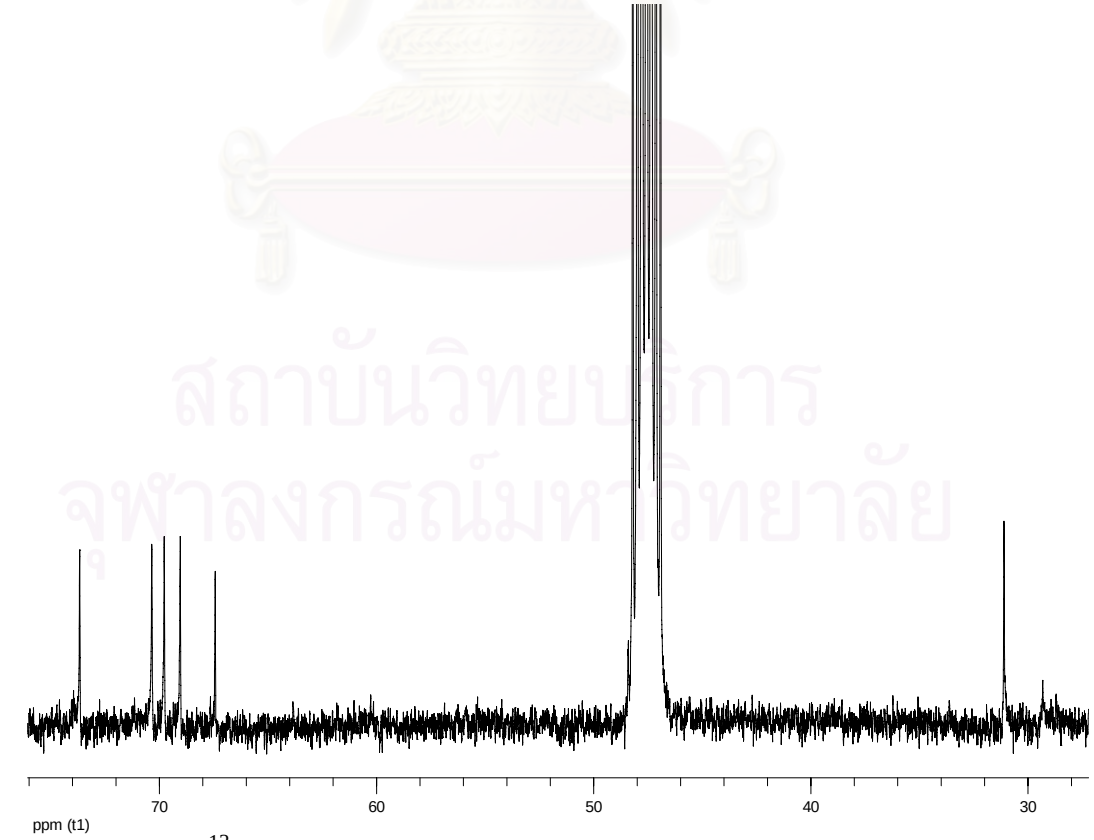

Figure 24. The ^{13}C NMR (CD_3OD) spectrum of **117**.

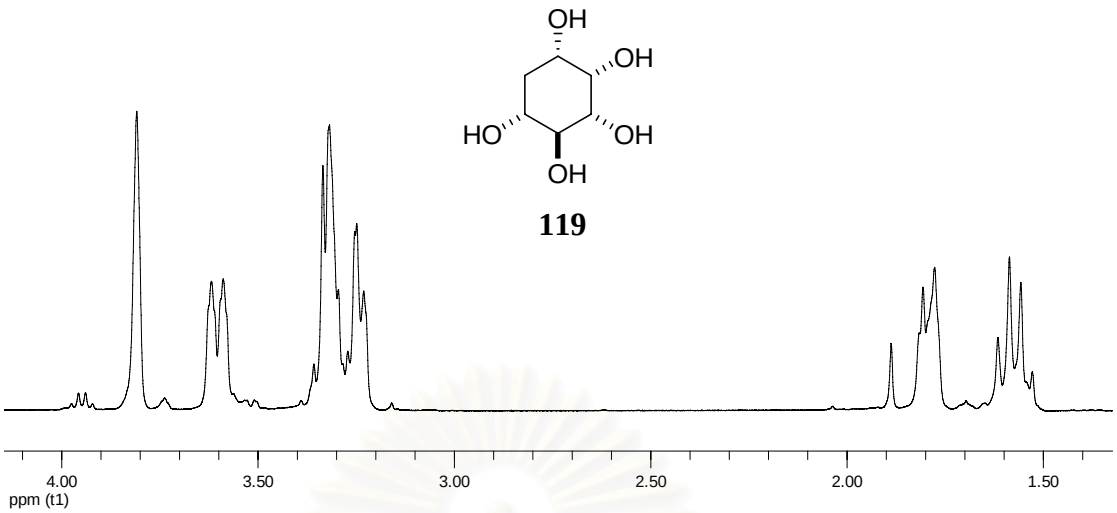

119

Figure 25. The ^{1}H NMR (D_2O) spectrum of **119.**

VITA

Ms. Wisuttaya Worawalai was born on July 15, 1983 in Mahasarakham province, Thailand. She graduated with Bachelor Degree of Science, majoring in Chemistry from Chulalongkorn University in 2006. In 2007, she further received a Master Degree in Department of Chemistry. During the course of study, she received the scholarship MUA & ADB under the Petroleum & Petrochemical Technology Consortium. Moreover, she was awarded first prize for the thesis research presentation from the Chulabhorn Graduate Institute (CGI) Award for Young Scientists 2008. In the same year, she also received the second prize poster presentation award of the 10^{th} National Graduate Research Conference at Sukothaithammatirat University.

Her present address is 135/18 Tumbon Tasongcon, Amphoe Muang, Mahasarakham, Thailand 44000.